Clinical Immunology 272 (2025) 110429

Contents lists available at ScienceDirect

Clinical Immunology

journal homepage: www.elsevier.com/locate/yclim

The immune response to SARS-CoV-2 in COVID-19 as a recall response susceptible to immune imprinting: A prospective cohort study

Daniel Alvarez-Sierra [a,**,1], Mónica Martínez-Gallo [a,b,c], Adrián Sánchez-Montalvá [d,e,f], Marco Fernández-Sanmartín [g,2], Roger Colobran [a,b,c], Juan Espinosa-Pereiro [d,e,f], Elísabet Poyatos-Canton [h,3], Coral Zurera-Egea [j], Alex Sánchez-Pla [k], Concepción Violan [l], Rafael Parra [m], Hammad Alzayat [g,2], Ana Vivancos [n], Francisco Morandeira-Rego [h], Blanca Urban-Vargas [h,4], Eva Martínez-Cáceres [c,i,j], Manuel Hernández-González [a,b,c], Jordi Bas-Minguet [h], Peter D. Katsikis [o], Aina Teniente-Serra [c,i,j], Ricardo Pujol-Borrell [b,c,n,*]

[a] *Translational Immunology Research Group, Vall d'Hebron Research Institute (VHIR), Campus Vall d'Hebron, Barcelona, Spain*
[b] *Immunology Department, Hospital Universitari Vall d'Hebron, Campus Vall d'Hebron, Barcelona, Spain*
[c] *Department of Cell Biology, Physiology, and Immunology, Universitat Autònoma Barcelona, Campus Vall d'Hebron and Campus Bellaterra, Barcelona, Spain*
[d] *Infectious Disease Department, Hospital Universitari Vall d'Hebron, Campus Vall d'Hebró, Barcelona, Spain*
[e] *International Health Program, Institut Català de la Salut, Vall d'Hebron Research Institute (VHIR), Campus Vall d'Hebron, Barcelona, Spain*
[f] *Centro de Investigación Biomédica en Red de Enfermedades Infecciosas (CIBERINFEC), Instituto de Salud Carlos III, Campus Vall d'Hebron, Barcelona, Spain*
[g] *Flow Cytometry Laboratory, Germans Trias i Pujol Research Institute (IGTP), Badalona, Barcelona, Spain*
[h] *Immunology Division, Bellvitge University Hospital, Hospitalet de Llobregat, Barcelona, Spain*
[i] *Immunology Department, Hospital Universitari Germans Trias I Pujol, Barcelona, Spain*
[j] *Immunology and Inflammation Research Group, Germans Trias i Pujol Research Institute (IGTP), Badalona, Barcelona, Spain*
[k] *Bioinformatics and Statistics Group, University of Barcelona, Barcelona, Spain*
[l] *Unitat de Suport a la Recerca Metropolitana Nord, Institut Universitari d'Investigació en Atenció Primària Jordi Gol (IDIAP Jordi Gol), Mataró, Barcelona, Spain*
[m] *Banc de Sang i Teixits, Hospital Universitari Vall Hebron, Barcelona, Spain*
[n] *Tumor Immunology and Immunotherapy Group, Vall Hebron Institut Oncology (VHIO), Campus Vall d'Hebron, Barcelona, Spain*
[o] *Dept. of Immunology, Erasmus University Medical Center, Rotterdam, the Netherlands*

ARTICLE INFO

Keywords:
SARS-CoV-2
COVID-19
Immune imprinting
Original antigenic sin
Plasmablast
cTfh
Spectral flow cytometry
Antibody-dependent-enhancement

ABSTRACT

The antibody response to SARS-CoV-2 does not follow the immunoglobulin isotype pattern of primary responses, conflicting with the current interpretation of COVID-19.

Methods: Prospective cohort study of 191 SARS-CoV-2 infection cases and 44 controls from the second wave of COVID-19. The study stratified patients by severity and analyzed the trajectories of SARS-CoV-2 antibodies and multiple immune variables.

Results: Isotype-specific antibody time course profiles to SARS-CoV-2 revealed a pattern of recall response in 94.2 % of cases. The time course profiles of plasmablasts, B cells, cTfh high-resolution subsets, and cytokines indicated a secondary response. The transcriptomic data showed that this cohort is strictly comparable to contemporary cohorts.

Conclusions: In most cases, the immune response to SARS-CoV-2 is a recall response. This constitutes a favorable scenario for most COVID-19 cases to be subjected to immune imprinting by endemic coronavirus, which, in turn, can influence the immune response to SARS-CoV-2.

* Correspondence to: R. Pujol-Borrell, Emeritus Professor of Immunology, Universitat Autònoma de Barcelona.
** Correspondence to: D. Alvarez-Sierra, "Sara Borrell" Postdoctoral Fellow, IDIVAL, Santander, Spain.
E-mail addresses: dalvarez@idival.prg (D. Alvarez-Sierra), ricardo.pujol@uab.cat (R. Pujol-Borrell).
[1] Group of Immunopathology, Marqués de Valdecilla Research Institute (IDIVAL), Cardenal Herrera Orio s/n, 39,011 Santander, Spain.
[2] Clinical Flow Cytometry Platform, Biomedical Dagnostic Center, Hospital Clinic, University of Barcelona, Villarroel 170, 08036 Barcelona.
[3] Immunology Laboratory, Pg. de Sant Joan de Déu, 2, 08950 Esplugues de Llobregat, Barcelona.
[4] Immunology Dpt, Immunology Department, Hospital Universitari Vall d'Hebron, Campus Vall d'Hebron, 08035 Barcelona, Spain.

https://doi.org/10.1016/j.clim.2025.110429
Received 20 November 2024; Received in revised form 12 January 2025; Accepted 14 January 2025
Available online 20 January 2025

1. Introduction

The COVID-19 pandemic has resulted in over 775 million confirmed cases and 7 million reported deaths worldwide as of October 2024 (WHO dashboard). Despite extensive research, one remaining area of uncertainty is the determinant of disease severity in COVID-19: whether it is primarily due to direct virus cytopathic effects, immune-mediated mechanisms, or a combination of both. A potential mechanism contributing to immune-mediated pathology in COVID-19 is immune imprinting (IP), also known as original antigenic sin. IP occurs when pre-existing immunity to related viruses interferes with the immune response to a new viral strain. In the case of SARS-CoV-2, this interference may stem from prior exposure to endemic Common Cold Coronaviruses (CCCoV).

Early reports on COVID-19 revealed an unexpected antibody response pattern, with IgA and IgG antibodies to SARS-CoV-2 proteins appearing simultaneously or even before IgM. [1,2] This observation contrasts with the typical primary immune response, where IgM consistently precedes IgG and IgA production. [3] A plausible explanation for this phenomenon is the interference of pre-existing cross-reactive immunity to endemic common cold coronaviruses (CCCoV) with the immune response to SARS-CoV-2 proteins. [4] This explanation aligns with evidence that many individuals unexposed to SARS-CoV-2 possess immunity to its proteins, which make them susceptible to IP. [5–8]' While retrospective studies have supported a significant role of IP in COVID-19 [4,9–11] definitely demonstrating IP and estimating its prevalence requires comparing pre- and post-COVID-19 paired serology samples and showing that the infection elicits a response to endemic CCCoV rather than to SARS-CoV-2. The scarcity of such paired samples in large prospective studies has limited investigations into this phenomenon.

In our comprehensive analysis of the immune response to SARS-CoV-2 conducted in a prospective cohort of unvaccinated COVID-19 patients during the second wave in the Barcelona metropolitan area, we found that approximately 95 % of patients had serological and cellular profiles typical of a recall immune response. Notably, these features were more pronounced in hospitalized cases compared to asymptomatic and mild cases. Given that IP occurs exclusively within the context of recall immune responses, our results suggest a potentially high prevalence of IP among COVID-19 patients.

2. Methods

2.1. Patients

The cohort of patients participating in the study was recruited at the participating hospitals (Hospital Universitari Bellvitge (HUB), Hospital Universitari Germans Trias i Pujol, (HUGTP) and Hospital Universitari Vall d'Hebron (HUVH) upon admission or at primary care centers at the first contact. In the latter scenario, health workers visited patients' homes to collect clinical and blood samples. Detected asymptomatic household sharing cases were recruited. Controls were selected among the Catalonian Blood and Tissue Bank (www.bst.cat) blood donors with a similar age and sex composition as the COVID-19 patients. All participants were informed of the project's objectives and signed the consent forms. Blood samples were collected into citrate, EDTA, sera separation, and Tempus® tubes (Becton-Dickinson Inc., NJ, USA).

A Research Electronic Data Capture (REDCap) database was generated to collect clinical and laboratory data. Information was introduced in 182 fields, including demographics, medical treatment history, comorbidities, Charlson's and SOFA indexes, initial symptoms, vital signs, physical examination, follow-up including oxygen requirements and therapy, and clinical chemistry data. The clinical data and blood samples were collected at the beginning and at two more time points. For all patients, the date of symptom onset was recorded and used to calculate "days from symptom onset" (DFSO) for each observation. The length of hospital stays (LOHS), ICU stay, oxygen supplementation, and ventilation support were also recorded.

Clinical severity categories were determined by the highest score during the follow-up period using the World Health Organization (WHO) 8-point COVID-19 disease clinical progression score. [12] The scores correspond to phenotypic categories: 0 no clinical or virological evidence of infection, 1: no limitation of activities, 2: limitation of activities, not requiring hospitalization, 3: hospitalized without oxygen requirement, 4: oxygen administered via a mask or nasal prongs, 5: non-invasive ventilation or high-flow oxygen, 6: intubation and mechanical ventilation, 7: ventilation and additional organ support and 8: deceased. In most analyses, patient classification was simplified as asymptomatic (score 1), mild (score 2), moderate (score 3–4), and severe (score of 5 to 8). Moderate and severe patients were all hospitalized.

2.2. Clinical laboratory and immunological tests

SARS-CoV-2 was detected by a real-time multiplex RT-PCR assay (Laplet 2019-nCoV Assay, Seegene, South Korea) in samples from nasal or pharyngeal swabs. Microbiological and clinical chemistry samples were processed by automatic analyzers integrated into continuous lines with automatic cold storage that ensured sample integrity. The levels of CCL2, CXCL10, GM-CSF, IFN-α, IFN-γ, IL-2, IL-4, IL-6, IL-7, IL-10, IL-12p70, IL-13, IL-15, IL-17 A, TGF-β1, TNF-α, granzyme-B and IL-1RA were measured in sera using the ELLA microfluidic platform (Biotechne®, Minneapolis, MN, USA). Calprotectin was measured by CLIA (Quantaflash®, Werfen, Barcelona, Spain).

Antibodies of the three immunoglobulin isotypes IgM, IgG, and IgA against SARS-CoV-2 main protease (M), nucleocapsid (NP), Spike (S) protein, and the RBD portion of the Spike protein were measured in serum samples using a commercial kit (SARS-COV-2 MULTIPLEX®, IMMUNOSTEP, Salamanca, Spain). [13] In some analyses, the sum of antibody levels for each isotype to Mpro, NP, and S proteins were used to score each individual's overall isotype-restricted response to SARS-CoV-2, annotated as SARS-CoV-2 IgA, SARS-CoV-2 IgG, and SARS-CoV-2 IgM. For type 1 IFN autoantibody measurement, ELISA was performed as previously described. [14] Positive controls and blanks were used as internal quality controls.

Whole blood was processed for high-dimensional flow cytometry, as reported. [15] Freshly obtained samples were stained with a 36-colour antibody panel (Supplemental Table 1) and analyzed using a 5-laser Aurora spectral flow cytometer (Cytek Biosciences). Unsupervised statistical inferences of the data were computed by OMIQ software (www.omiq.ai). UMAP was used for dimensionality reduction, and flowSOM was used for clustering.

For transcriptomic profiling, 250 ng of total RNA from PBMC, quantified using the NanoDrop 2000 (Thermo Scientific), was directly hybridized (at 65 °C for 18 h) with a mixture of biotinylated capture probes and fluorescently labeled reporter probes complementary to target sequences., Gene expression values were first normalized to the positive controls and then normalized according to the nCounter Expression Data Analysis Guide (mAN-C0011–02). The nCounter® Human Immunology Host Response Panel was used for this study (https://nanostring.com/products/ncounter-assays-panels/immunology/host-response).

2.3. Statistical analysis

Analysis was conducted in the R environment version 4.3.2 and R Studio. The distribution of variables was determined to apply the appropriate type of test. All tests considered two-tailed distributions to calculate the *p*-value, adjusted by Bonferroni except where otherwise stated; p values <0.05 were considered significant. In LOESS regression curves, 95 % CI are represented unless otherwise noted. Sex as a biological variable was considered in every statistical analysis but reported separately only when significant differences were detected. The study

was carried out or supervised by the bioinformatic and statistical analysis unit of Vall d'Hebron Research Institute (VHIR) (https://vhir.vallhebron.com/ca/suport-la-recerca/unitat-destadistica-i-bioinformatica-ueb).

2.4. Ethical

The institutional ethics board approved this project of the institutions (HUB: 120/20; HUGTP: ImmuneProfile-COVID19 REF.CEI PI-20-218 and HUVH: Protocol number VH, PR(AG)242/2020).

3. Results

3.1. Features of the Barcelona COVID second-wave cohort

The final cohort included 191 COVID-19 cases and 44 blood donors as controls recruited in 2020, during the second wave of COVID-19 in Barcelona, before the vaccination campaign started in January 2021. [16] Of the patients, 38 were asymptomatic, 49 mild, 64 moderate, and 40 severe. The study's design is depicted in Fig. 1. The inclusion criteria were being above 18 years of age, having a confirmed virological diagnosis of SARS-CoV-2 by PCR, and agreeing to participate. In the case of healthy blood donors, cases with a history of clinical COVID-19 or a positive serological test in our assay were excluded.

Table 1 and 2 show the details of cases by period, severity, samples, and tests. For the analysis of results, we have considered three periods based on the days from symptoms onset (DFSO), DFSO1 0–7 days, DFSO2 8–20 days, and DFSO3 21–107 days. The number of patients per period was 101, 128, and 60, and the number of samples per period was 139, 188, and 65, respectively. Of the 483 samples, only 13 (2.7 %) were collected at DFSO >60. Due to financial constraints, cytokines were measured in 67 %, and RNA profiles (Nanostring®) in 15 % of the samples, which were selected to represent each severity and period group.

Out of the 106 hospitalized patients, 31 (29.2 %) required admission to the ICU, and the median length of stay in the hospital (LOSH) was 15 days [7–25]. Their ICU stays averaged 14 days [7–27]. The demographic, clinical, and laboratory data are in Table 1, 2, 3 and 4. The overall mortality during the follow-up period was 6/191 (3.1 %).

4. Analysis of the antibody response to the SARS-CoV-2 proteins

4.1. The time course profiles correspond to a recall immune response and are associated with severity but not with the presence of Type-1 IFN autoantibodies

We analyzed the serological response to Mpro, NP, Spike (S), and Spike RBD (RBD) in 473 samples from 190 patients and 44 controls. The values were standardized using the control group's IQR3.

In period DFSO1, the antibody response showed significant

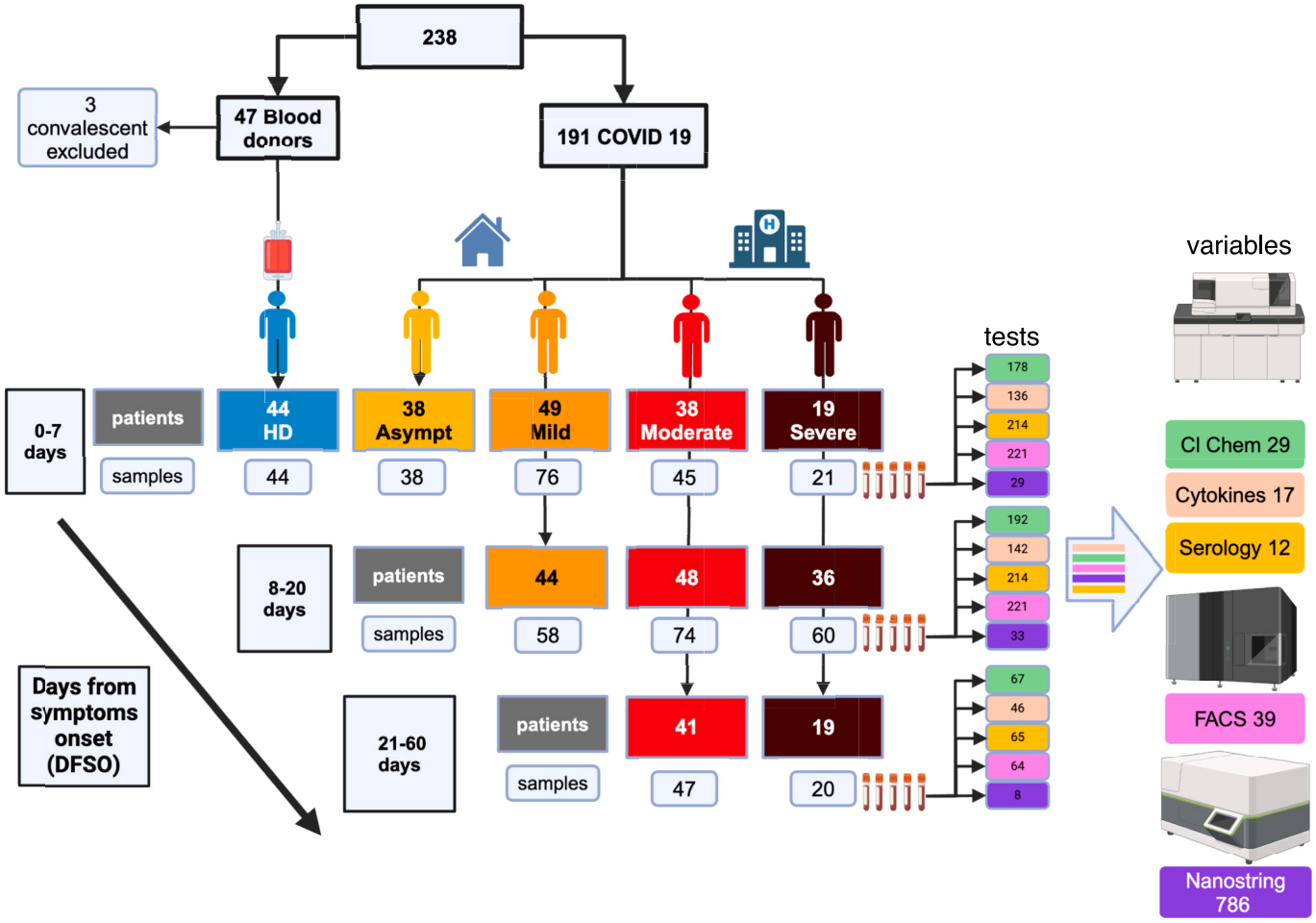

Fig. 1. Study design and patient flow chart. The figure summarizes the patient groups, the timeline, and the number of variables measured in each group. Clinical data were available from all 235 individuals, but due to financial limitations, cytokine and Nanostring tests were applied to 67 % and 15 % of the samples, respectively (see text). DFSO, days from symptoms onset; Asympt, asymptomatic cases. Large colored boxes, patient numbers; small pale blue boxes, sample numbers; colored boxes on the right edge, number of samples by period and type of test; the colored boxes under the equipment icons give the test colour code. (For interpretation of the references to colour in this figure legend, the reader is referred to the web version of this article.)

Table 1
Patients and sample distribution across the follow-up periods.

		Periods																	
		DFSO1 or DFSO_A or DFSO_C (0–7 days)						DFSO2 (8–20 days)						DFSO3 (21–107 days)					
		Patients	Samples					Patients	Samples					Patients	Samples				
Groups, total patients		n	Cl Chem	Cytokines	Serology	Flowcyt	Nanostr	n	Cl Chem	Cytokines	Serology	Flowcyt	Nanostr	n	Cl Chem	Cytokines	Serology	Flowcyt	Nanostr
Control	44	44	NA	24	38	44	6	NA	NA	NA	NA	NA	NA	NA	NA	NA	NA	NA	NA
Asympt	38	38	38	28	37	37	6	NA	NA	NA	NA	NA	NA	NA	NA	NA	NA	NA	NA
Mild	49	49	74	47	74	76	10	44	58	41	58	57	10	ND	ND	ND	ND	ND	ND
Moderate	64	38	45	24	45	45	3	48	74	56	73	70	13	41	47	30	46	45	5
Severe	40	19	21	13	20	19	4	36	60	45	57	58	10	19	20	16	19	19	3
Totals	235	188	178	136	214	221	29	128	192	142	188	185	33	60	67	46	65	64	8

This table summarizes the period of patient enrollment, observation, samples, and variables measured in them. In the top periods, in the bottom table the samples in the order they were taken, A, B and C. Notice that 26 moderate and 21 severe contributed their samples in period DFSO2; also that while 107 contributed three samples, 34 two and 14 one. See text section results "Features of the Barcelona COVID second-wave cohort" for details and justification. Cl.Chem = Clinical Chemistry; Flowcyt = Flowcytometry; Nanostr = Nanostring®.

Table 2
Patients' contribution per period.

DFSO1			
Severity	Patients	Samples	Patients that contributed two samples
Control	44	44	0
Asymptomatic	38	38	0
Mild	49	76	27
Moderate	38	45	7
Severe	19	21	2
Total	188	224	
DFSO 2			
Mild	44	58	14
Moderate	48	73	25
Severe	36	58	22
Total	128	189	
DFSO 3			
Moderate	41	47	6
Severe	19	20	1
Total	60	67	

This table clarifies the number of patients that contributed more than one sample per a given time period in the trajectory regression analysis.

differences in control versus all severity group patients, except for anti-RBD (Supplemental Fig. S1a and b). Interestingly, the only significant IgM response during this period was to the Spike protein. The differences became more evident in the following DFSO periods when the response to RBD and IgM isotype antibodies became detectable (see Supplemental Fig. S2a–d). Although the highest responses were initially observed in moderate patients, they resembled those of severe patients during the follow-up. Responses were also detected in asymptomatic patients but were only significant for anti-S IgG.

The antibody response was more prolonged in patients with more severe symptoms with a considerably later peak response, especially for anti-RBD and IgG isotype antibodies (Fig. 2a and b). To better visualize antibody response time course profiles, we plotted severity-stratified data using LOESS regression curves summarizing each isotype's antibody response (Fig. 2c). Two key observations emerged: 1) IgM responses did not appear before IgA or IgG, neither initially nor at the peak of the response. 2) Antibody levels decreased in mild patients between 13 and 16 days but only after 30 and 47 days for moderate and severe patients.

This lack of an IgM response to SARS-CoV-2 preceding the IgG and IgA responses, as expected in an immune response to a new pathogen, suggested that in most patients, the response was, at least in part, a recall response. However, as in a LOESS regression some cases with a primary response may be missed, we looked for primary responders by selecting patients who, during the initial seven days, had a normalized level of antibody above 1.5 for the IgM isotype and below 1.5 for the IgG or IgA isotype. The sum of Mpro, NP, and S antibodies for each isotype and patient was used for this filter. Eight out of 139 cases (5.8 %) were identified. They corresponded to four mild and four asymptomatic patients, all from the primary care sub-cohort, none requiring hospital admission (age 52 range 29–71, five females, and three males). Representative profiles are shown in Fig. 2d. These primary responders later developed good IgG and IgA antibody responses. The interpretation of these results is that in this COVID-19 cohort, the majority develop a recall type of immune response to SARS-CoV-2 proteins.

An expected feature of a response to a new pathogen is a coordinated immune response to the pathogen's different antigens. In our cohort, the responses to the SARS-CoV-2 Mpro and NP proteins are coordinated, but not the response to S and especially to the RBD (Supplemental Fig. S3 blue boxes). As the receptor binding domain (RBD) of SARS-CoV-2 differs significantly from other circulating coronaviruses, a delayed and slow response to RBD would indicate the need for a primary immune

Table 3
Summary of demographic and clinical data.

	Healthy	Asympt	Mild	Moderate	Severe	All	*p* among groups
Demographic	N (%)	N (%)	N (%)	N (%)	N (%)	N (%)	
	44 (18.7)	38 (16.2)	49 (20.9)	64 (27.2)	40 (17.0)	235	
Blood Bank	44 (100)	NA	NA	NA	NA	44 (18.7)	NA
Primary Care	0 (0)	38 (100)	47 (95.9)	5 (7.8)	1 (2.5)	91 (38.7)	NA
HUB	NA	NA	0 (0)	20 (31.3)	18 (45.0)	38 (16.2)	NA
HUGTP	NA	NA	1 (2.0)	22 (34.4)	9 (22.5)	32 (13.6)	NA
HIUVH	NA	NA	2 (4.1)	18 (28.2)	10 (26.3)	30 (12.8)	NA
Age (median IQR)	50 [45–59]	41 [36–56]	48 [35–62]	53 [44–60]	68 [55–73]	54 [41–69]	**2.12e-06**
Age, severe vs other groups, p values (Wilcox)	3.41e-06	1.42e-04	3.90e-04	7.00e-03	NA	NA	
Sex							
Male	18 (40.9)	24 (63.2)	28 (57.1)	22 (34.4)	10 (25.0)	102 (43.4)	**0.003**
Female	26 (59.1)	14 (36.8)	22 (44.9)	43 (70.0)	28 (70.0)	133 (56.6)	
Toxic Habits							
Smoker	0	4 (10.5)	4 (8)	1 (1.6)	2 (5.0)	11 (5.8)	0.257
Alcohol	0	1 (2.6)	1 (2)	5 (7.8)	1 (2.5)	8 (4.3)	0.447
Comorbidities							
Psychiatric disease	0	3 (7.9)	7 (14.3)	5 (7.8)	4 (10.0)	19 (9.9)	0.674
Diabetes	0	2 (5.3)	3 (6.1)	15 (23.4)	9 (22.5)	29 (15.2)	**0.010**
Immunosuppression	0	0 (0)	0 (0)	2 (3.1)	4 (10.0)	6 (3.1)	0.594
Solid Cancer	0	2 (5.3)	1 (2)	7 (10.9)	5 (12.5)	15 (7.9)	0.197
Active Cancer	0	0 (0)	0 (0)	0 (0)	2 (5.0)	2 (1.0)	0.052
Hypertension	0	8 (21.1)	6 (12.2)	23 (35.9)	16 (40.0)	53 (27.7)	**0.006**
Heart failure	0	0 (0)	0 (0)	4 (6.3)	2 (5.0)	6 (3.1)	0.151
Lung Disease	0	0 (0)	2 (4.1)	10 (15.6)	6 (15.0)	18 (9.4)	**0.019**
Chronic Kidney Failure	0	1 (2.6)	0 (0)	5 (7.8)	3 (7.5)	9 (4.7)	0.183
Liver Cirrhosis	0	0 (0)	0 (0)	0 (0)	1 (2.6)	1 (0.5)	0.284
Neurologic Disease	0	0 (0)	1 (2)	1 (1.6)	1 (2.5)	3 (1.6)	0.192
Charlson's Score	NA	0 [0, 1.8]	0 [0,2]	1 [0,3]	2.5 [2, 4]	1 [0,3]	**3.90e-06**
Prior Medication							
Anticoagulants	NA	0 (0)	2 (4.1)	3 (4.7)	2 (5.0)	7 (3.7)	0.150
Corticosteroids	NA	0 (0)	0 (0)	3 (4.7)	3 (7.5)	6 (3.1)	**0.029**
Immunosuppression	NA	0 (0)	0 (0)	1 (1.6)	1 (2.5)	2 (1.0)	**0.029**
Statins	NA	3 (7.9)	1 (2.0)	31 (48.4)	11 (27.5)	46 (24.1)	**0.002**
Angiotensin convertase inhibitors	NA	4(10.5)	4 (8.2)	11 (17.2)	4(10.0)	23(12.0)	0.469
Angiotensin receptor II blockers	NA	5(13.1)	4(8.2)	3 (4.7)	10(25.0)	22(11.5)	**0.013**
Clinical Presentation							
Fever	NO	0 (0)	12 (24.4)	52 (81.2)	31 (77.5)	31 (16.2)	**6.336e-19**
Weight loss	NO	0 (0)	1 (2.04)	3 (4.68)	0 (0)	4 (2.1)	0.288
Malaise	NO	1 (100)	38 (77.5)	29 (45.3)	20 (50)	88 (46.1)	**1.535e-10**
Cough	NO	0 (0)	26 (53.0)	42 (65.6)	21 (52.5)	89 (46.6)	**1.622e-09**
Dyspnoea	NO	0 (0)	0 (0)	27 (42.1)	24 (60)	51 (26.7)	**1.995e-13**
Expectoration	NO	0 (0)	0 (0)	2 (3.12)	1 (2.5)	3 (1.6)	**0.455**
Haemoptysis	NO	0 (0)	0 (0)	1 (1.56)	0 (0)	1 (0.5)	**0.573**
Pleuritic Chest Pain	NO	0 (0)	0 (0)	2 (3.12)	3 (7.5)	5 (2.6)	**0.105**
Rhinorrhoea	NO	0 (0)	2 (4.08)	1 (1.56)	0 (0)	3 (1.6)	**0.356**
Anosmia	NO	1 (2.63)	8 (16.3)	16 (25)	6 (15)	30 (15.7)	**0.032**
Cacosmia	NO	0 (0)	0 (0)	1 (1.56)	2 (5)	3 (1.6)	0.219
Odynophagia	NO	0 (0)	0 (0)	7 (10.9)	2 (5)	9 (4.7)	**0.020**
Myalgia	NO	0 (0)	2 (4.08)	15 (23.4)	12 (30)	29 (15.2)	**7.54e-05**
Nausea	NO	0 (0)	1 (2.04)	9 (14.0)	6 (15)	16 (8.4)	**0.012**
Vomits	NO	0 (0)	0 (0)	8 (12.5)	1 (2.5)	9 (4.7)	**0.004**
Diarrhoea	NO	0 (0)	1 (2.04)	16 (25)	12 (30)	29 (15.2)	**1.557e-05**
Confusion	NO	0 (0)	0 (0)	0 (0)	3 (7.5)	3 (1.6)	**0.009**
SpO2/FiO2, median IQR	NA	NA	466 [461–471]	442 [340–461]	361 [271–457]	277 [165–339]	**0.028**

NA, not applicable; *p* among groups: Kruskal-Wallis test; significant values in bold. HUB, Hospital Universitari Bellvitge, Hospital Universitari Germans Trias i Pujol, Hospital Universitari Vall d'Hebron.

response distinct from the response to other SARS-CoV-2 proteins.

A reported observation is that in COVID-19, the antibody response titer correlates positively with the disease's severity. In our cohort, maximal antibody titers were indeed associated with severity on the five-point scale (control, asymptomatic, mild, moderate, and severe, Fig. 3a and b). This correlation was also found when stratified by WHO scores (Supplemental Fig. S4a and b). The interpretation of the association of severity with the serological response is that antibodies do not protect against severity during the early stages of COVID-19, notwithstanding their protective role as RBD-neutralizing antibodies against re-infection. [17]

As anti-type I IFN autoantibodies have been associated with the severity of COVID-19 [14], we measured anti-IFN-alpha and anti-IFN-omega autoantibodies. Only 10 of the 232 (4.9 %) COVID-19 cases and two of the 44 controls (4.5 %) were positive. Of these ten positive cases, one was asymptomatic, three moderate, three severe, and one deceased; three were female, and four were males (including the deceased). This small number of positive cases indicated that anti-type I

Table 4
Summary of laboratory data.

	Control	Asymptomatic	Mild	Moderate	Severe	
Patients	44	38	49	64	40	
Clinical chemistry	Median [IQR]	Median [IQR]	Median [IQR]	Median [IQR]	Median [IQR]	p. adjusted
Hb	15.00 [13.50, 16.02]	14.30 [13.62, 15.07]	14.20 [13.35, 14.95]	13.35 [12.35, 14.70]	13.20 [12.10, 14.22]	4.33E-05
WBC	6.30 [5.16, 7.77]	5.65 [4.55, 6.47]	4.50 [3.70, 5.90]	5.28 [4.10, 6.62]	7.45 [6.07, 12.66]	1.90E-07
Basophils 10e9/L	0.00 [0.00, 0.10]	0.00 [0.00, 0.00]	0.00 [0.00, 0.00]	0.00 [0.00, 0.01]	0.00 [0.00, 0.02]	6.14E-03
Basophils %	0.70 [0.50, 0.92]	0.50 [0.30, 0.70]	0.50 [0.30, 0.60]	0.30 [0.20, 0.50]	0.20 [0.10, 0.30]	1.90E-07
Eosinophils 10e9/L	0.10 [0.10, 0.20]	0.10 [0.00, 0.10]	0.10 [0.00, 0.10]	0.00 [0.00, 0.02]	0.00 [0.00, 0.01]	1.90E-07
Eosinophils %	2.05 [1.67, 3.20]	1.45 [0.83, 2.30]	1.20 [0.55, 1.85]	0.20 [0.00, 0.70]	0.00 [0.00, 0.10]	1.90E-07
Lymphocytes 10e9/L	1.90 [1.50, 2.42]	1.95 [1.40, 2.38]	1.60 [1.30, 1.85]	1.00 [0.86, 1.42]	0.86 [0.50, 1.20]	1.90E-07
Lymphocytes %	30.40 [25.65, 33.95]	35.70 [30.65, 41.08]	34.70 [28.00, 41.90]	21.30 [13.10, 26.20]	9.40 [5.25, 16.95]	1.90E-07
Monocytes 10e9/L	0.50 [0.40, 0.60]	0.50 [0.32, 0.70]	0.50 [0.40, 0.60]	0.45 [0.30, 0.60]	0.40 [0.30, 0.62]	2.79E-01
Monocytes %	7.80 [6.97, 9.05]	8.45 [7.30, 11.42]	10.20 [8.90, 13.35]	8.80 [5.55, 11.10]	5.05 [3.77, 7.82]	1.90E-07
Neutrophils 10e9/L	3.40 [2.95, 4.85]	2.75 [2.20, 3.50]	2.30 [1.80, 3.00]	3.54 [2.69, 4.72]	7.50 [4.56, 11.44]	1.90E-07
Neutrophils %	58.50 [53.48, 62.30]	50.80 [46.10, 57.95]	49.40 [44.60, 58.50]	68.85 [58.68, 80.03]	82.75 [78.05, 89.25]	1.90E-07
Platelets 10e9/L	218.50 [188.50, 255.25]	197.50 [172.50, 234.75]	197.00 [169.50, 214.50]	214.00 [164.50, 278.25]	236.00 [181.25, 327.00]	2.42E-02
C Reactive protein mg/dL (0.03–0.5 mg/dL)	ND	0.23 [0.15, 0.95]	0.39 [0.20, 1.46]	6.18 [2.41, 10.76]	11.91 [7.55, 19.55]	1.90E-07
Calprotectin	ND	1.50 [0.90, 1.96]	1.17 [0.91, 1.78]	4.80 [3.01, 9.00]	9.78 [6.14, 22.76]	1.90E-07
D-dimer (0–243 ng/mL)	ND	306.00 [251.00, 408.00]	326.00 [213.00, 517.00]	309.00 [250.00, 612.00]	417.00 [266.50, 958.25]	1.53E-01
Ferritin (25–400 ng/mL)	ND	120.50 [36.75, 283.50]	173.00 [66.50, 316.75]	415.00 [215.50, 1130.00]	738.00 [508.50, 1383.75]	1.90E-07
LDH (120–246 IU/L)	ND	171.00 [157.25, 199.25]	174.00 [158.50, 201.25]	250.00 [197.50, 331.50]	389.00 [304.50, 480.00]	1.90E-07
ALT 10–49 IU/L)	ND	20.00 [14.00, 32.00]	21.00 [15.00, 33.00]	36.00 [17.00, 61.50]	35.00 [21.75, 49.25]	1.13E-03
AST (8–34 IU/L)	ND	23.00 [18.25, 27.75]	25.00 [21.00, 32.25]	39.00 [24.50, 55.00]	39.00 [31.50, 55.00]	1.90E-07
Total Bilirubin (0.3–1.2 mg/dL	ND	0.42 [0.31, 0.53]	0.46 [0.36, 0.62]	0.50 [0.41, 0.70]	0.53 [0.36, 0.58]	1.99E-02
Triglycerides (43–200 mg/dL)	ND	85.00 [69.50, 121.25]	107.00 [74.00, 133.00]	131.00 [100.00, 158.50]	134.50 [89.75, 201.75]	3.88E-04
Creatinine (0,67–1.17 mg/dL)	ND	0.82 [0.71, 1.02]	0.82 [0.69, 0.99]	0.81 [0.67, 0.94]	0.82 [0.71, 0.94]	9.60E-01
Urea (17–42 mg/dL)	ND	29.40 [25.35, 35.70]	30.00 [25.80, 36.60]	33.00 [26.38, 48.45]	48.90 [39.90, 57.50]	1.90E-07
Fibrinogen ((2.39–6.1 g/L)	ND	4.63 [3.96, 5.26]	4.47 [3.91, 4.95]	6.00 [4.00, 7.00]	6.00 [5.00, 7.00]	3.54E-06
Prothrombin Time INR	ND	1.10 [1.04, 1.13]	1.10 [1.05, 1.16]	1.02 [0.98, 1.12]	1.07 [1.00, 1.13]	4.82E-02
Anti-SARS-CoV-2 Serology						
Anti-SARS-CoV-2 Mpro IgM	33.26 [22.03, 47.63]	39.10 [24.23, 58.06]	33.31 [25.12, 68.87]	76.69 [28.52, 202.40]	71.48 [27.81, 246.80]	1.35E-03
Anti-SARS-CoV-2 NP IgM	19.79 [10.30, 36.46]	22.87 [12.06, 40.19]	20.17 [11.95, 52.20]	49.58 [17.15, 153.28]	44.92 [19.82, 191.47]	5.66E-04
Anti-SARS-CoV-2 Spike IgM	11.26 [7.73, 16.63]	18.14 [11.35, 23.69]	18.27 [10.64, 50.39]	195.79 [32.00, 419.62]	166.40 [19.37, 597.09]	1.90E-07
Anti-SARS-CoV-2 RBD IgM	28.30 [18.08, 50.42]	31.68 [18.74, 51.56]	34.24 [22.47, 57.83]	27.30 [18.18, 56.10]	28.44 [13.35, 67.82]	6.45E-01
Anti-SARS-CoV-2 Mpro IgG	104.62 [79.80, 140.57]	131.61 [98.43, 213.75]	141.66 [103.37, 251.88]	2366.32 [218.92, 8961.47]	3802.74 [255.20, 17,061.04]	1.90E-07
Anti-SARS-CoV-2 NP IgG	87.82 [52.94, 147.42]	108.90 [67.80, 299.94]	119.68 [65.33, 219.93]	1523.34 [213.28, 6132.72]	1675.92 [198.03, 14,891.76]	1.90E-07
Anti-SARS-CoV-2 Spike IgG	352.43 [172.59, 519.99]	482.34 [413.13, 781.45]	363.83 [287.60, 674.92]	1182.96 [479.80, 2882.23]	1409.81 [675.78, 3069.88]	1.90E-07
Anti-SARS-CoV-2 RBD IgG	151.80 [99.39, 189.06]	166.19 [141.64, 197.79]	169.66 [127.47, 230.83]	174.49 [124.02, 258.31]	206.29 [150.35, 267.33]	2.09E-02
Anti-SARS-CoV-2 Mpro IgA	63.42 [53.66, 78.82]	73.47 [52.11, 156.64]	82.32 [53.31, 147.56]	1863.08 [141.85, 7094.48]	1950.15 [170.74, 21,127.41]	1.90E-07
Anti-SARS-CoV-2 NP IgA	47.75 [38.01, 66.72]	60.97 [37.51, 128.13]	65.71 [39.42, 145.72]	2233.86 [139.40, 8282.62]	1494.22 [165.56, 22,643.54]	1.90E-07
Anti-SARS-CoV-2 Spike IgA	89.72 [71.30, 133.01]	99.82 [64.31, 290.57]	219.47 [88.11, 307.64]	2401.77 [267.93, 10,810.81]	3780.36 [478.96, 9936.22]	1.90E-07
Anti-SARS-CoV-2 RBD IgA	97.75 [89.98, 110.80]	101.33 [83.12, 117.93]	101.37 [91.10, 122.64]	108.62 [89.57, 152.74]	101.66 [89.19, 148.74]	2.96E-01
Cytokines and chemokines						
IFN-alpha	0.00 [0.00, 0.20]	3.52 [0.30, 25.55]	15.75 [2.17, 37.62]	15.25 [2.63, 33.75]	2.05 [0.05, 15.85]	8.68E-07
IFN-gamma	0.79 [0.64, 0.97]	2.28 [1.08, 6.73]	3.04 [1.69, 5.01]	9.61 [3.04, 24.89]	3.50 [2.10, 9.84]	1.90E-07
TNF-alpha	12.41 [9.91, 15.28]	20.95 [16.53, 24.30]	21.94 [18.42, 27.83]	21.30 [16.84, 30.80]	21.57 [18.75, 27.06]	1.90E-07
IL-6 pg/ml	3.06 [2.33, 4.46]	3.44 [2.67, 9.15]	5.12 [3.46, 15.40]	33.85 [19.82, 56.38]	37.20 [16.10, 107.02]	1.90E-07
IL-1RA pg/ml	365.02 [269.41, 504.56]	581.58 [443.75, 922.75]	940.33 [539.00, 1548.07]	1727.37 [1281.84, 2839.75]	2190.32 [1377.82, 3004.16]	1.90E-07

(*continued on next page*)

Table 4 (*continued*)

	Control	Asymptomatic	Mild	Moderate	Severe	
Patients	44	38	49	64	40	
Clinical chemistry	Median [IQR]	Median [IQR]	Median [IQR]	Median [IQR]	Median [IQR]	p. adjusted
IL-7 pg/ml	13.89 [10.13, 16.30]	14.15 [10.70, 18.85]	15.57 [10.61, 18.24]	21.90 [13.12, 32.41]	39.30 [25.55, 55.57]	3.58E-07
IL-12p70 pg/ml	1.16 [0.29, 2.75]	2.45 [1.68, 2.84]	2.13 [1.18, 2.93]	1.77 [1.24, 2.11]	1.60 [1.05, 2.15]	2.03E-02
IL-10 pg/ml	2.98 [1.85, 3.43]	4.46 [3.80, 8.32]	5.48 [3.63, 8.25]	12.10 [8.74, 17.90]	19.20 [11.75, 23.15]	1.90E-07
IL-13 pg/ml	6.74 [4.06, 11.20]	8.60 [3.32, 16.40]	9.33 [6.43, 15.65]	7.20 [5.62, 18.62]	8.75 [5.18, 15.72]	2.95E-01
IL-15 pg/ml	2.83 [2.09, 4.00]	3.53 [2.87, 4.98]	4.98 [3.50, 6.39]	5.35 [4.19, 7.35]	5.52 [4.61, 6.79]	3.58E-07
IL-17 A pg/ml	1.17 [0.69, 2.00]	2.41 [1.71, 3.14]	2.76 [2.03, 3.90]	2.57 [2.10, 4.54]	2.58 [1.57, 3.91]	6.67E-05
IL-2 pg/ml	0.15 [0.08, 0.30]	0.30 [0.22, 0.45]	0.44 [0.32, 0.64]	0.84 [0.51, 2.04]	0.76 [0.48, 1.03]	1.90E-07
IL-4 pg/ml	0.66 [0.53, 0.78]	0.50 [0.35, 0.61]	0.58 [0.45, 0.79]	0.72 [0.47, 1.04]	0.70 [0.57, 0.86]	2.42E-02
GM-CSF pg/ml	1.62 [1.26, 2.04]	3.10 [2.29, 3.71]	2.32 [1.45, 3.04]	2.13 [1.58, 3.37]	2.98 [1.71, 4.07]	4.38E-04
TGF beta-1 pg/ml	114.50 [73.12, 151.25]	163.00 [104.00, 196.75]	169.50 [133.00, 229.25]	125.00 [47.15, 172.50]	188.00 [103.50, 289.50]	3.52E-03
CCL2 pg/ml	438.01 [338.12, 556.64]	542.00 [423.25, 675.00]	613.00 [488.55, 919.00]	653.00 [486.65, 866.25]	883.00 [489.00, 1576.64]	1.19E-03
CXCL10 pg/ml	133.50 [119.94, 165.00]	466.00 [290.50, 930.00]	878.00 [584.75, 1478.25]	1742.91 [1177.00, 2278.00]	2371.00 [1645.33, 3604.50]	1.90E-07
GRANB pg/ml	15.60 [11.30, 18.80]	33.30 [26.35, 46.75]	42.20 [26.92, 64.93]	43.35 [26.00, 65.07]	36.60 [27.55, 51.55]	1.90E-07

IFN autoantibodies were not an essential determinant of severity in this cohort and did not interfere significantly with the analysis and its interpretation.

4.2. Cytokine time course profiles are consistent with a recall immune response to SARS-CoV-2

To identify which cytokines were driving the humoral response, we analyzed the correlations of cytokines with the antibody titers at each period and severity group. The most interesting observation is the significant negative correlation of IFN-γ, especially with the serological response in moderate patients at DFSO2; it is known that there is a mutual inhibitory effect of IFN-γ/IL-2 and IL-4/IL-13 in the initial polarization of the immune response, which may explain these results [18] (Supplemental Fig. S5). The positive correlation of IL-7 with antibody titers in severe and moderate patients is probably due to its secretion to compensate for lymphopenia, which correlates negatively with antibodies to SARS-CoV-2. [19] Overall, the pattern of cytokines with peaks at DFSO2 for mild and at DFSO3 for moderate and severe cases suggest a mixture of early and late secondary immune responses.

5. Blood cell populations in COVID-19

As reported, neutrophils were relatively expanded in COVID-19 patients, and lymphocytes were reduced. [20] To better analyze B and T cell populations, we have used both the absolute number and the proportion of a subset within each lymphocyte's main compartment. The most striking change was in plasma/plasmablast cells, which increased in all severity categories (Supplemental Fig. S6). The spectral flow cytometric analysis of total blood resolved 46 populations further split into 197 clusters. For the interpretation, three degrees of resolution were considered: low (7 subsets), medium (46 subsets), and high (197 clusters). Only those contributing to discern between a primary and a recall response are included in this report.

5.1. Time course profiles of plasmablast subsets show features of a recall response

Plasmablasts and plasma cells, from here on PBs, as defined by CD38 +, CD27+, HLA-DR++, sIg, and variable CD19, were split into four main clusters: IgA+, IgG+, IgM+, and sIg^- and three low-abundance clusters: IgM + IgA+, IgM + IgG +, and long-life plasma cells (LLPC), according to the UMAP (Fig. 4a and b). The number of PBs rose rapidly in moderate and severe patients, surpassing at DFSO1 day three the maximal levels of mild patients at day seven; their peak exceeded the peak in mild patients by a factor of two and three, respectively (Fig. 4c). In some severe patients, PBs made up to 60 % of lymphocytes (Supplemental Fig. S7a).

From the trajectories, it is inferred that IgA+ PB was the dominant subset during the incubation period and was replaced by sIg- PB on DFSO day 3 (Fig. 4d and e). The parallelism of total PB cells and antibody titer trajectories suggests that PBs cells are the source of at least some of these antibodies (Supplemental Fig. S7b). A negative correlation of PBs with Th1 cytokines IFN-gamma and IL-2 and a positive correlation with IL-10 and IL-7 is expected in an immune response (Supplemental Fig. S8).

5.1.1. Interpretation

The first IgA wave of plasmablasts originates from memory B in upper airway mucosa secondary lymphoid organs (SLO) that cross-react with CCCoV rather than from a primary response. [21]

5.2. Time course profiles of the B lymphocyte subset in COVID-19 patients are consistent with a recall response

Flow cytometry identified 32 clusters of B lymphocytes summarized in 13 subsets and eight unclassified minor clusters (Fig. 5 and Supplemental Fig. S9). The total B cell trajectory differs from that of leukocytes and T cells; still, with time, their shifts show parallelism (Fig. 5b). Subset trajectories are very variable (Fig. 5d–h). Switched and memory subset trajectories differed markedly among severity groups and also when compared by period and severity (Supplemental Table 2).

The B cell subset correlation analysis with the serological response revealed a distinct pattern. In mild patients, the correlations are positive and significant during the initial eight days (DFSO1) for B cell subsets involved in the early phase of the response, i.e., transitional, naïve activated, IgM-only memory, and CD24++ immature IgG memory (Fig.6a and Supplemental Fig. S10). Consistently, the trajectories of memory and switched subsets show a delay (Fig. 6b & c).

5.2.1. Interpretation

The capture of cross-reactive antigens by CCCoV-specific memory B cells would delay the recruitment of naïve B cells in moderate and severe cases. A fresh, specific response to SARS-CoV-2 would be initiated only when a large amount of antigen reaches the SLO. The B cell trajectories point to a predominant recall response.

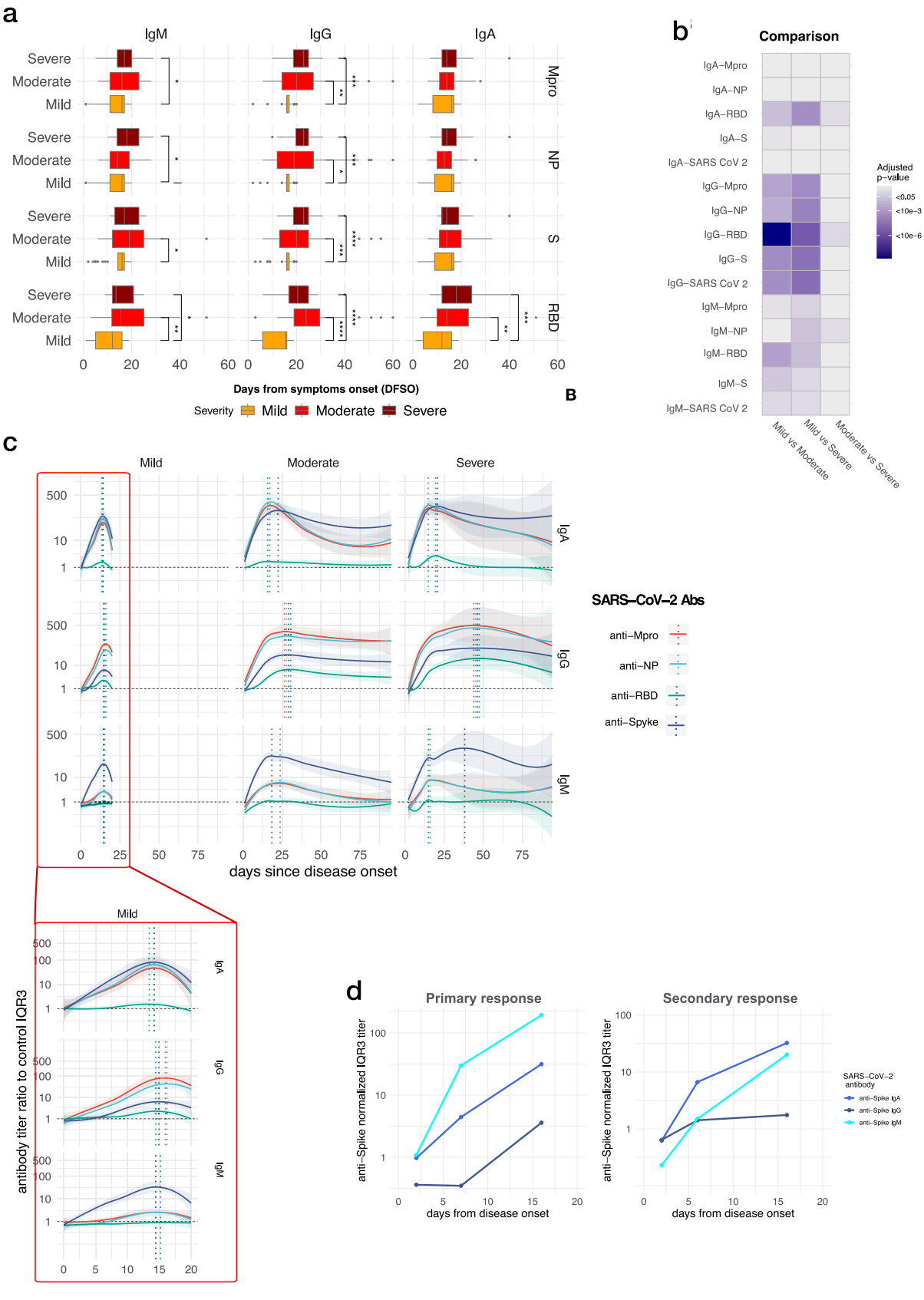

(caption on next page)

Fig. 2. Time course profiles of SARS-CoV-2 antibody levels. (a) The peak levels of the 88 cases from which we collected three samples during the initial 60 days are plotted against time. There's a noticeable delayed peak for moderate and severe cases compared to mild cases. Median ± IQR. (b) A heatmap summarizes the significance level of the comparisons, highlighting clustering in the IgG category and the comparison between mild vs. severe and mild vs. moderate cases. (c) LOESS regression curves with 95 % confidence intervals of the normalized antibody titers of 392 samples from 190 COVID-19 cases are shown. The vertical dotted lines represent the maximal titer, and the horizontal lines represent the established normal level for data normalization. In the red box inset, the time scale has been zoomed to visualize the trajectories during the initial 20 days. It is evident that the first response is IgA, followed by IgG and IgM. The responses have already started to decrease at DFSO 13–15 days. The rise of the IgM antibody regression curve never precedes the other isotype curves in moderate or severe patients. The maximal IgG titer is reached between 43 and 47 days for moderate and severe patients. It's also noteworthy that the predominant antigen for IgM isotype antibodies is Spike, while IgA, NP, Mpro, and NP predominate over Spike for IgG. Responses to RBD were predominantly IgG. (d) Representative patients for primary and secondary responses; only responses to Spike have been represented. (For interpretation of the references to colour in this figure legend, the reader is referred to the web version of this article.)

5.3. Time course profiles of cTfh cells in COVID-19 patients are consistent with a recall response

Circulating Tfh (cTfh) reflects the activity of Tfh cells in the SLO. [22] It correlates with antibody response, but their trajectory differs from total T cells or typical effector memory CD8 cells (Fig. 7a). cTfh can be classified as cTfh-naïve, cTfh1, cTfh17, cTfh2, and cTfh1 activated, [22] identified in the corresponding UMAP (Fig. 7b). All cTfh clusters were significantly higher in asymptomatic and mild than in moderate and severe (Fig. 7c). The association of low cTfh with severity was not explained by age or sex in the multivariate model. Notably, despite the low number of cTfh cells, the rise in antibodies to SARS-CoV-2 was earlier and faster in moderate and severe hospitalized patients than in mild not-hospitalized patients, suggesting that these antibodies are produced by memory B cells that do not require Tfh (Supplemental Fig. S11a and b).

5.3.1. Interpretation

The overall pattern of the cTfh response indicates that in hospitalized patients, the antibody response is dominated by memory B cells that do not require Tfh. In asymptomatic and mild Tfh, Tfh activates naïve B cells that generate new antibodies.

5.4. Nanostring transcriptomic signature

Seventy samples from 33 patients, representative in terms of age, sex, and severity, were selected for transcriptomic profiling. The results were stratified for the analysis in 60 gene groups.

The strong BCR signaling signatures in asymptomatic patients are of interest because other techniques detected only slight changes in this group (Supplemental Fig. 12). In the immune memory panel, the stronger signal for CD45RA in asymptomatic and mild patients with the differential pattern in the lymphocyte trafficking highlights the different regulation of the immune responses in asymptomatic and mild vs the hospitalized moderate and severe. It is also remarkable that there is an interferon response signature in the asymptomatic and some mild cases. The results are consistent with an immune response, mainly recall in moderate and severe patients but with more elements of a primary response in asymptomatic and mild.

The panels of genes associated with myeloid and monocyte cell activation and the expected IL-1 signaling pathway show some of the main differences related to severity (Supplemental Fig. S13).

These results are similar to many transcriptomic profiles of COVID-19 patients and indicate that our cohort is representative of COVID-19. [23]

6. Discussion

At the beginning of the COVID-19 pandemic (early 2020), over 50 % of hospitalized patients developed pneumonia, with many requiring oxygen therapy and intensive care unit admission. The mortality rate among these patients was in our hospitals 16.1 %. [20]. We, like others, attempted to develop predictive algorithms based on immunological variables to help triage the patients. We identified different response immunotypes [24], but the algorithms had to include clinical severity data to be clinically helpful. [20,25] These shortcomings highlighted the limitations of available tools for identifying the immunological determinants of disease severity.

One possible immunological factor of severity that escaped then our analysis was the occurrence of immune imprinting (IP) that can interfere with the immune response [26] This possibility has been discussed in several studies [6,27,28] since evidence that many individuals possessed antibodies and memory T cells to CCCoV that cross-react with SARS-CoV-2 proteins was produced early in the pandemic. [6,29] A recent study established a link between pre-existing immunity to CCCoV and COVID-19 severity. [10] Despite this evidence, IP has not been incorporated into the central paradigm to explain severe COVID-19. [17,30] Our research addresses this gap by investigating whether the immune response in COVID-19 patients exhibits characteristics of a recall response, which is a prerequisite for IP. Our analysis was triggered by the simple observation that, in our cohort, the IgM response to SARS-CoV-2 antigens did not precede the IgA and IgG responses as expected, and by the lack of coordination of the responses to the different SARS-CoV-2 antigens. The first of these anomalies was already detected in the 2020 reports of antibody response to SARS-CoV-2, but the focus was then on applying serology to diagnosis. [1,2,31,32]

In this paper, we report that the time course profiles of antibody responses to SARS-CoV2, when analyzed in depth, together with the clinical course and the shifts in plasmablasts, B cell, and cTfh subpopulations indicate that in most cases, the immune response to SARS-CoV-2 is a recall response. Interestingly, the features of recall response were more evident in the two categories of patients that required hospitalization. This constitutes a favorable scenario for IP but does not demonstrate the expansion of endemic coronavirus reactive memory B cells that would constitute robust evidence of IP.

Our study is prospective. The clinical data of all cases were curated by their physicians; patients were from the same geographical, received health care from a single health provider (Institut Català de la Salut, (ICS, https://ics.gencat.cat), and all immunological methodologies had been previously validated; all these aspects make the data of this study particularly robust.

A close analysis of the antibody response trajectories by SARS-CoV2 protein and isotype, stratified by patients' severity, offers additional evidence of a recall immune response. The fast and dominant IgA responses to the Mpro, NP, and Spike suggest a mucosal origin from memory resident T and B. [33–35] That the IgM response, even if weaker, is dominated by the response to Spike, whose sequence is more distant from that of CCCoV, suggests that the recruitment of naïve cells, even if late, does contribute to mounting the response to SARS-CoV-2 specific epitopes. This vigorous late IgG response may originate from lymph nodes draining the lower respiratory airways.

The main limitation of our study is that we did not measure antibodies to endemic coronavirus in samples obtained before and after the COVID-19 episode as required to demonstrate immune imprinting. However, since a study in a simultaneous cohort from Barcelona showed a strong back-boosting effect to conserved but not variable regions of OC43 and HKU1 beta coronaviruses spike proteins when comparing pre- and post-COVID-19 samples, we consider that most probably the same

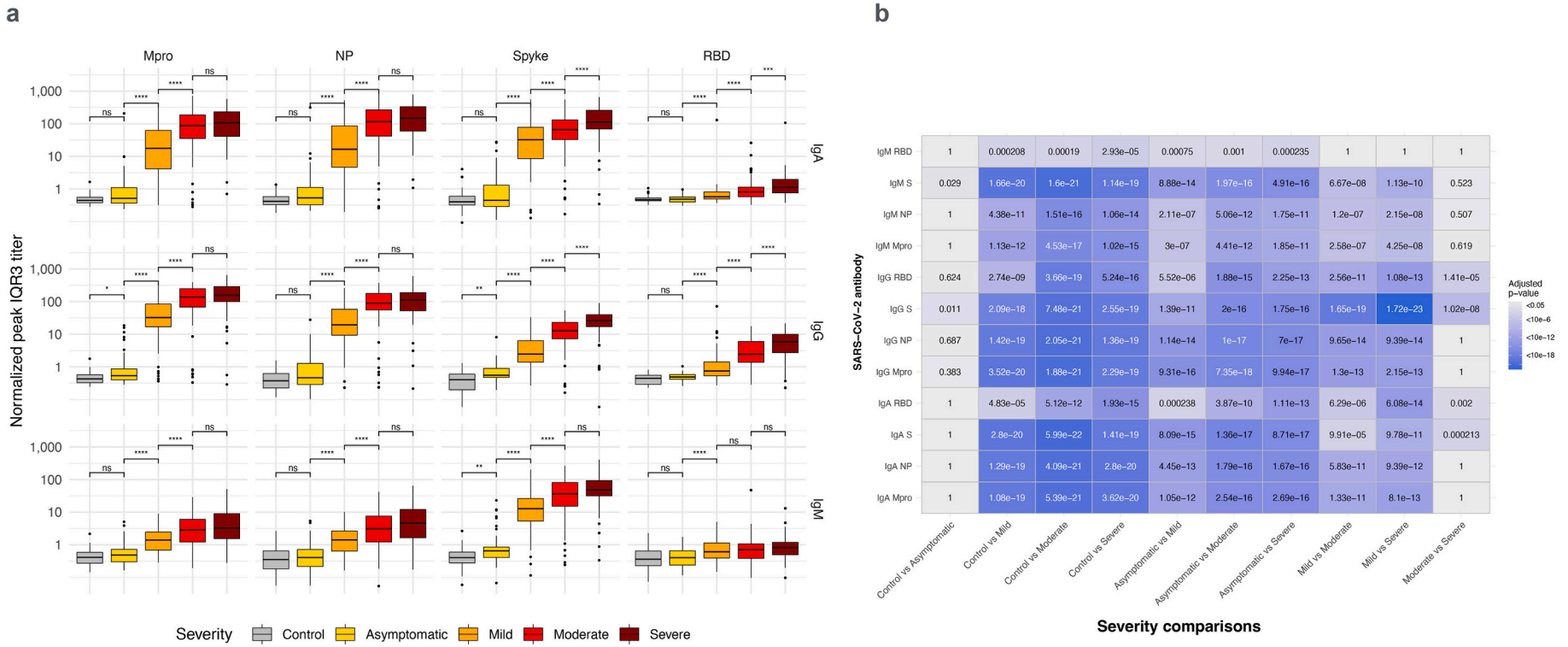

Fig. 3. The intensity of the antibody response increases with severity. (A) Maximal antibody levels were compared for the clinical cases with three serological measurements plus control and asymptomatic cases. Notice how the antibody levels significantly increase with the severity. Median ± IQR. (B) Heatmap summarizing plot comparisons, Pairwise Wilcoxson test. See supplemental Fig. S3 for the same analysis but with the WHO eight-point scale.

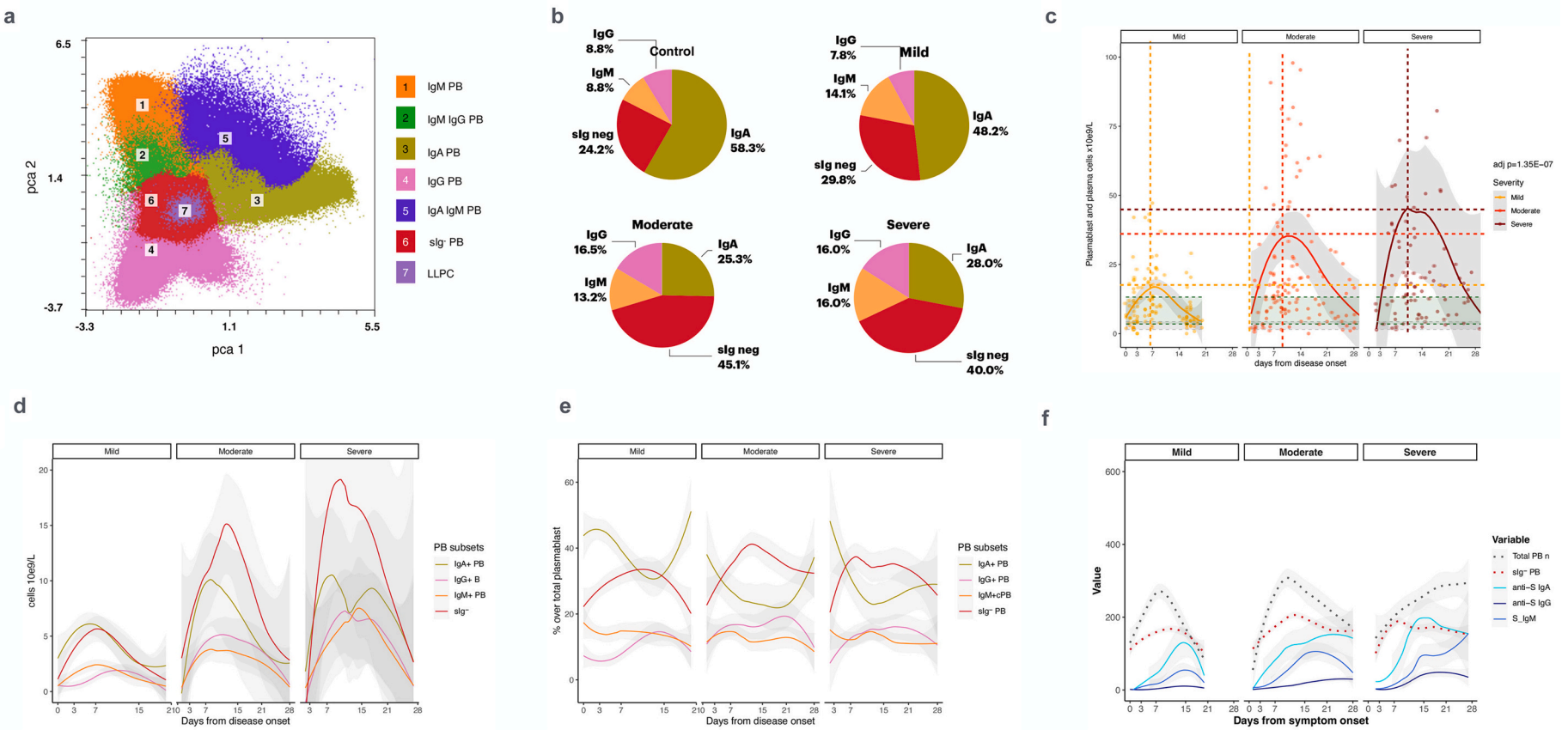

Fig. 4. Plasmablast (PB) expansion within the WBC, lymphocyte populations, and subset analysis. (a) UMAP of plasmablast clusters; (b) Distribution of plasmablast among the four main subpopulations, IgA+, IgG+, IgM+, and sIg$^-$ in controls and the three severity categories. The expansion of PB is due to the rise in the number of sIg$^-$ PBs. (c) LOESS trajectories of total plasmablasts during the initial 28 days by severity categories. The horizontal dashed lines indicate the different levels of the maximal number of cells. The vertical dashed lines indicate the day the maximal level is reached for each category, highlighting the remarkable differences in their respective trajectories. The magnitude of PB's absolute expansion can be appreciated (d and e). The comparison of PB subset trajectories shows that their expansion is due to the sIg$^-$ PB subset. (f) Composite trajectory plot showing total PBs and sIg- PB trajectories and normalized antibody titers to SARS-CoV-2 S proteins. Values in the y-axis are cell numbers or normalized antibody titers; cell numbers were transformed to place them in the same range as serological titers. LLP, long life plasma cell; sIg- PB, surface immunoglobulin negative plasmablast.

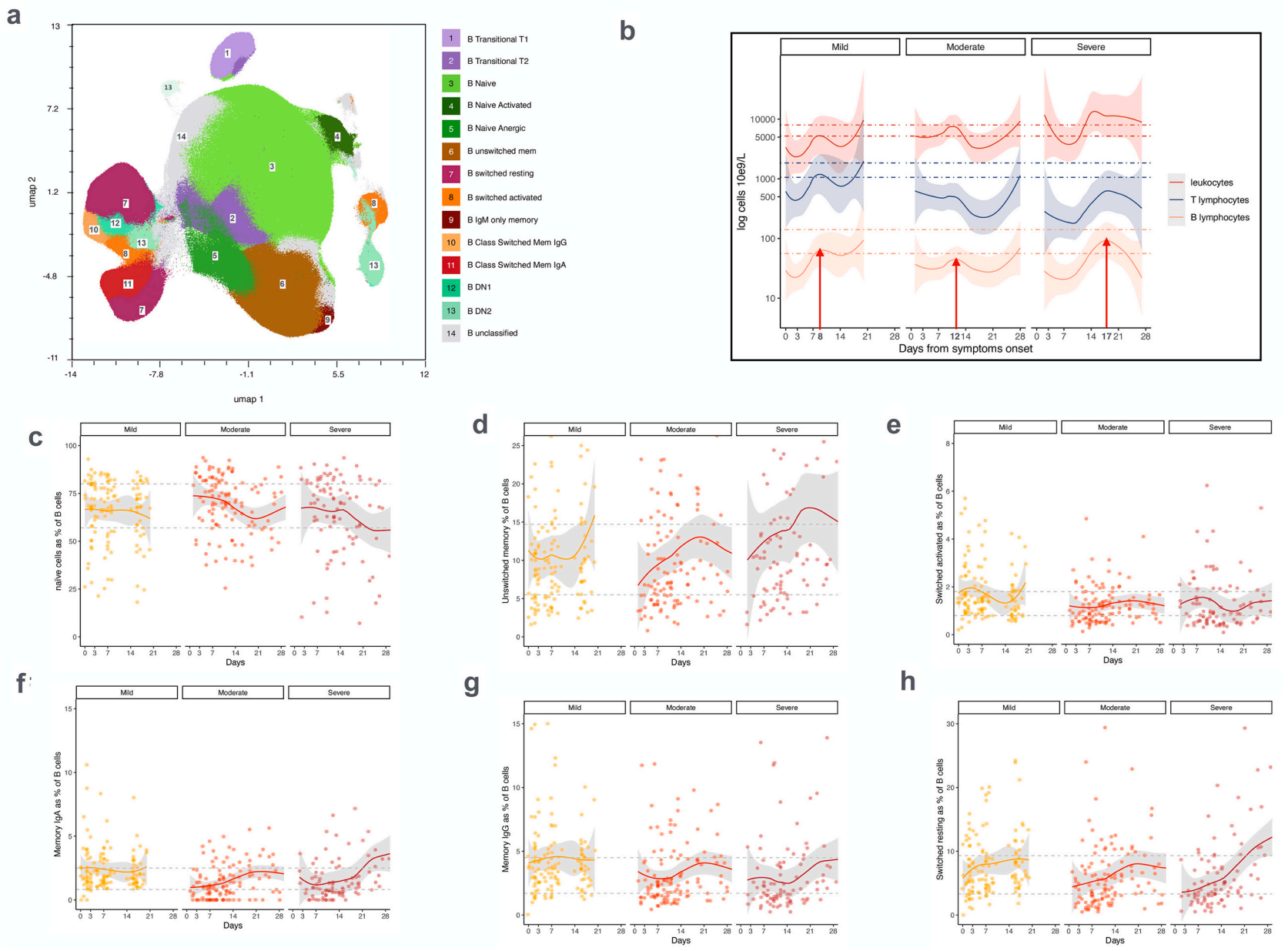

Fig. 5. Time course profiles of B cell subsets. (a) UMAP of B cells displays the distribution of the 13 subpopulations summarizing 32 clusters. (b) LOESS trajectory of leucocytes, T and B lymphocytes counts for the three categories of clinical COVID-19. In plots c-h, the samples are mild 130, moderate 134, and severe 89. The y-axis represents the percentage of total B cells. (c) Naïve; (d) unswitched memory; (e) Switched activated; (f) Memory IgA; (g) Memory IgG; (h) switched resting B cells. The dashed lines indicate quartiles 1 and 3 of the distribution of the values in the control population for each subpopulation. By comparing each population (c-h) with (b), it is noticeable that the circulating B cell population is less reduced compared to total lymphocytes and that recovery is earlier in the less severely ill patients. DN, double negative.

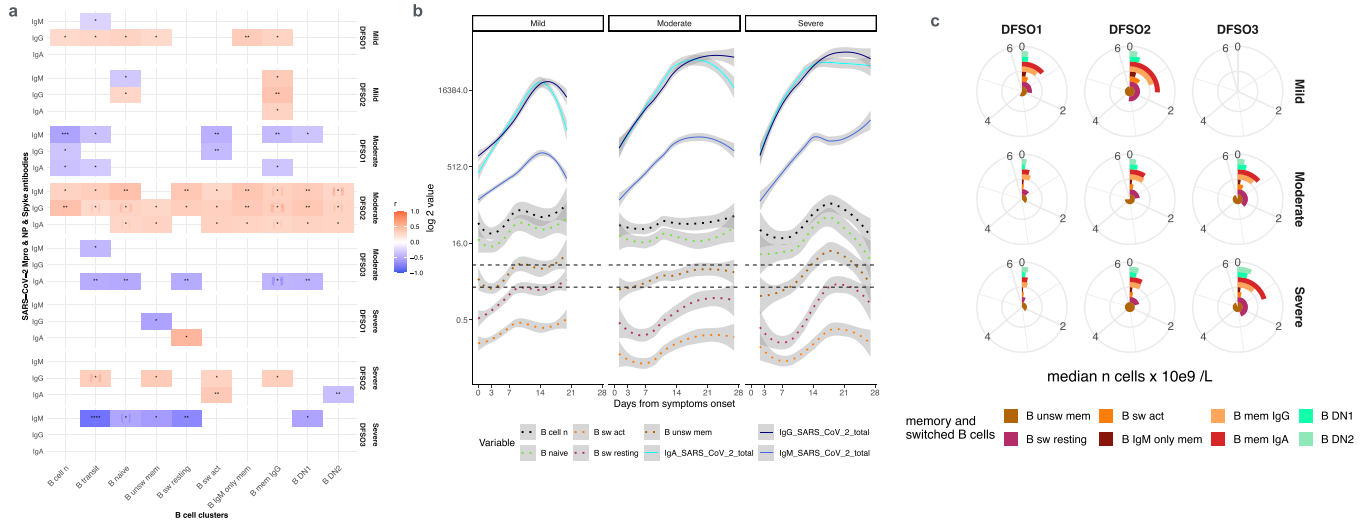

Fig. 6. Time course profiles of B cell subsets associated with a recall immune response. (a) Heatmap summarizing the correlation (Spearman) of B cell subsets and serological response by severity and follow period. DFSO, days from symptoms onset. DFSO1 0–7. DFSO2 8–20, DFSO3 21–107. (b) LOESS regression trajectories comparing B cell subsets and antibodies to SARS-CoV-2 proteins. (c) Ring doughnut charts comparing the distribution of the B cell subset along the follow-up period by severity. See text for details. Notice that the inner circles represent the most abundant subpopulations. DN, doble negative;sw, switched; unsw, unswitched; mem, memory.

results could be extrapolated to our cohort. [8] In their article, Aydillo et al. consider their data evidence for IP [8]. Another limitation is that we did not test the sera for neutralizing SARS-CoV-2 antibodies, but it has been repeatedly shown that they correlate closely with anti-RBD antibodies. [36]

IP may be highly deleterious to the host, which is why it is also known as original antigenic sin [26]. The predominant immune response is directed to the dominant epitopes of the original immunizing virus, and the effectors generated, both antibodies and CD8 T cells, having low affinity for the new epitopes, are inefficient, resulting in a more severe infection. The conceptual cellular and molecular basis is well understood; memory B and T cells recognize/capture the cross-reactive protein/peptide, and as they have a lower threshold for activation, they dominate the response, preventing the activation of naïve cells that may carry more specific receptors for the new epitopes. However, because cross-reactive antibodies and T cells may have some protective effect, IP does not always determine a severe infection. [37] In addition, as the amount of viral antigens reaching the lymph nodes increases with time, a primary specific response eventually takes off and leads to the control of the infection. Besides interfering with the primary response, IP can be associated with antibody-dependent enhancement [26]. Observed in some viral infections, e.g., dengue, and occasionally after vaccination, its occurrence of in COVID-19 has been discussed, and it has been a concern for developing the SARS-CoV-2 vaccines.

In conclusion, our analysis of the trajectories of a broad selection of immunological variables in a prospective cohort of the second wave of COVID-19 indicates that, in most cases, the immune response to SARS-CoV-2 functions as a recall response. While this does not constitute direct evidence of IP, it underscores the possibility that IP is an important immunological determinant influencing disease severity.

Data sharing

Supplemental tables contain the additional data required to re-analyze the data: the xlsx file with the transcriptomic data will be made available on request.

Author contribution

D. A-S, M. M-G, A. S-M, J. B-M, A. T-S, M. H-G, and R. P-B conceived and designed the project. A. S-M designed the redcap database. M.A. F-S and H. A performed the high-dimension flow cytometry data analysis and interpretation. J.A.E-P., E.P-C. C. Z-E, F.M-R, and B. U-V collected samples and clinical data from hospitalized patients, while C.V. organized it from the primary care centers and visiting teams. R.P. organized the control group. A. S-P. conducted the statistical and bioinformatic analysis. E.M-C., M. M-G, and C.V. reviewed and contributed to the manuscript drafts. P.K. reviewed the pre-final versions and suggested insightful analyses. A.V. conducted the Nanostring analysis n. D. A-S ran the project's logistics, conducted the cytokine measurements, and performed some statistical and bioinformatic analyses. R.P-B supervised the project, carried out the global data analysis and interpretation, wrote the manuscript, and prepared tables and figures.

Credit authorship contribution statement

Daniel Alvarez-Sierra: Writing – review & editing, Validation, Methodology, Investigation, Formal analysis, Data curation. **Mónica Martínez-Gallo:** Writing – review & editing, Validation, Conceptualization. **Adrián Sánchez-Montalvá:** Writing – review & editing, Validation, Formal analysis, Data curation, Conceptualization. **Marco Fernández-Sanmartín:** Writing – review & editing, Validation, Software, Investigation, Formal analysis, Conceptualization. **Roger Colobran:** Writing – review & editing, Validation, Investigation. **Juan Espinosa-Pereiro:** Writing – review & editing, Validation, Data curation. **Elísabet Poyatos-Canton:** Validation, Data curation. **Coral Zurera-Egea:** Validation, Data curation. **Alex Sánchez-Pla:** Validation, Supervision, Software, Formal analysis. **Concepción Violan:** Writing – review & editing, Validation, Project administration, Methodology. **Rafael Parra:** Validation, Investigation. **Hammad Alzayat:** Validation, Investigation, Data curation. **Ana Vivancos:** Validation, Investigation. **Francisco Morandeira-Rego:** Validation, Data curation. **Blanca Urban-Vargas:** Validation, Data curation. **Eva Martínez-Cáceres:** Writing – review & editing, Validation, Investigation, Formal analysis, Conceptualization. **Manuel Hernández-González:** Validation, Supervision, Resources, Methodology, Formal analysis, Conceptualization. **Jordi Bas-Minguet:** Writing – review & editing, Validation, Resources, Investigation, Conceptualization. **Peter D. Katsikis:** Writing – review & editing, Validation, Conceptualization. **Aina Teniente-Serra:** Writing – review & editing, Validation, Investigation, Funding acquisition, Data

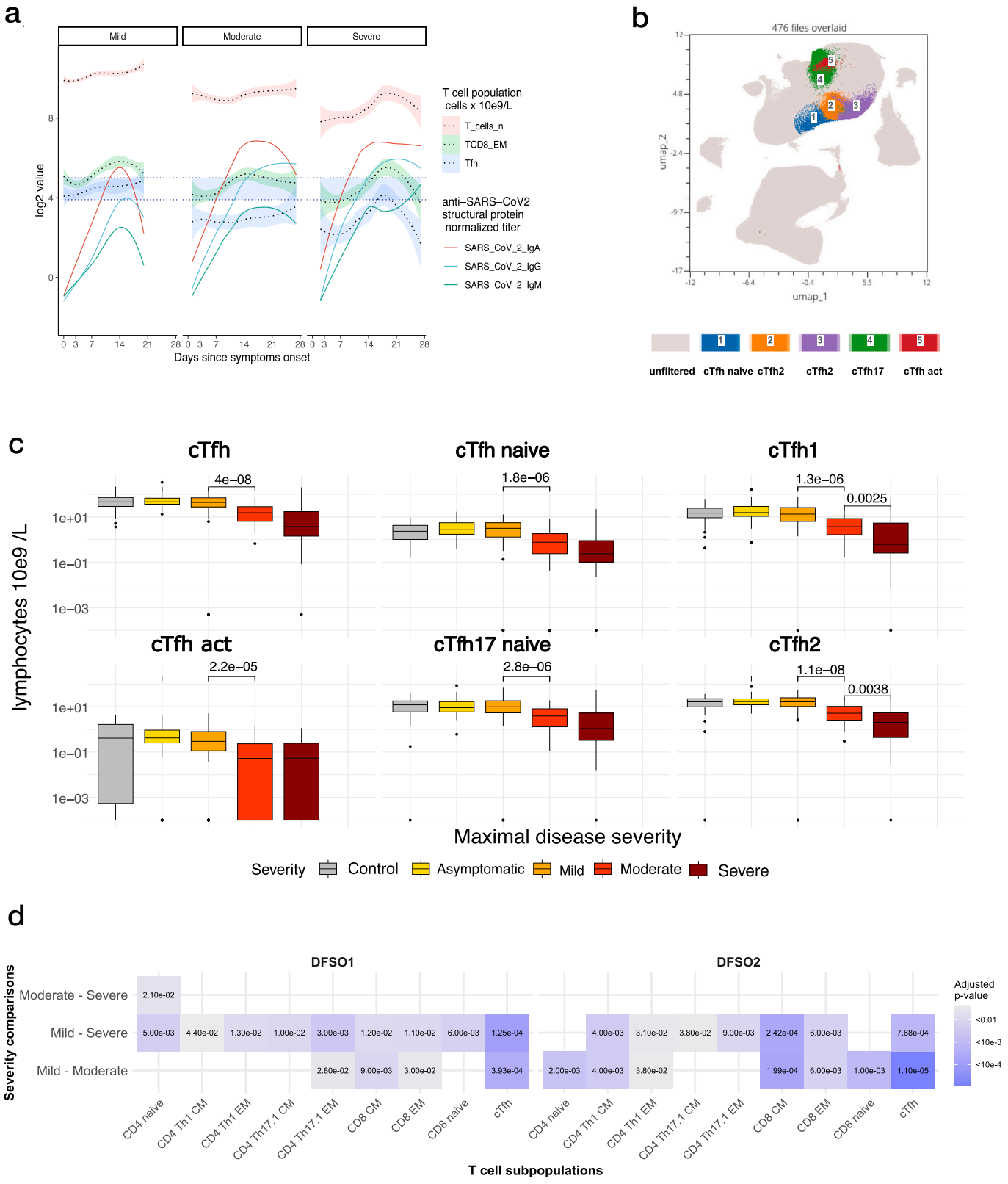

Fig. 7. cTfh and clusters. (a) Comparison of LOESS trajectories of total T lymphocyte number, CD8 EM, and cTfh with the LOESS trajectories of normalized antibody to SARS structural proteins. The 95 % CI of trajectories is represented; the blue ribbon helps to visualize how cTfh in mild remains consistently above the levels in moderate and severe patient groups. Notice that in moderate and severe, the antibody titers rise despite a lower number of cTfh. Median ± IQR. (b) UMAP shows the distinct cTfh clusters within the T cell distribution. (c Both total Tfh (top left panel) and each cTfh subcluster have significantly different values distributions for mild vs moderate (Wilcoxon test p. adjusted Benjamin-Hochberg). (d) Heatmap showing the pairwise comparison of T cell subsets among the severity groups. cTfh distribution is the most significantly different (Wilcoxon test p. adjusted Benjamin-Hochberg). CM, central memory; EM effector memory. (For interpretation of the references to colour in this figure legend, the reader is referred to the web version of this article.)

curation, Conceptualization. **Ricardo Pujol-Borrell:** Writing – review & editing, Writing – original draft, Visualization, Validation, Supervision, Resources, Project administration, Methodology, Investigation, Funding acquisition, Formal analysis, Data curation.

Declaration of competing interest

All authors declare that they have no conflicts of interest.

Data availability

Data will be made available on request.

Acknowledgments

This study was funded by grants COV20/00416, Cov20/00654, and COV20/00388 to RP-B, AT-S, and JB-M respectively, from Instituto de Salud Carlos III (ISCIII), Ministry of Economy and Competitiveness, Spain, co-financed by the European Regional Development Fund (ERDF). D.Á-S was the recipient of a doctoral fellowship from the Vall d'Hebron Research Institute (VHIR), Barcelona, Spain, up to 2023 and from 2024 by a ISCIII postdoctoral fellowship, "Sara Borrell," CD23/0011. A.S-M was supported by a ISCIII postdoctoral fellowship, "Juan Rodés" (JR18/00022). Bioinformatics analysis has been carried out in part in the Statistics and Bioinformatics Unit (UEB) at Vall d'Hebron Research Institute (VHIR).

The authors thank all the patients and health staff of the Hospital Universitari Vall d'Hebron, Hospital Universitari Bellvitge, and Hospital Universitari Germans Trias i Pujol and Primary Care Units who endured the pandemic and did their best to overcome the successive waves of COVID-19 in Barcelona, an experience that none of us would ever forget. The authors are grateful to Sergio Navarro Velázquez and Mario Framil Seoane from Hospital Universitari Bellvitge and to Arturo Llobell Uriel and Joan Roig Sanchis from Hospital Universitari Vall d'Hebron for their support in reviewing patients' records within the general Immunoprofile COVID-ICS project. Dr. Isabel Novoa-Garcia and Ms. Sheyla Pascual Martin for their invaluable help in organizing and maintaining the COVID-19 collection in the HUVH BioBank. To Ms. Adelaida Parada and the administrative and technical staff of immunology laboratories at the participating hospitals that collected and organized the COVID-19 patient samples for review by the medical personnel of this study.

During the preparation of this work the author(s) used Grammarly and Perplexity to improve syntaxis and readability but reviewed and edited the content as needed.

Appendix A. Supplementary data

Supplementary data to this article can be found online at https://doi.org/10.1016/j.clim.2025.110429.

References

[1] Q.-X. Long, B.-Z. Liu, H.-J. Deng, G.-C. Wu, K. Deng, Y.-K. Chen, P. Liao, J.-F. Qiu, Y. Lin, X.-F. Cai, D.-Q. Wang, Y. Hu, J.-H. Ren, N. Tang, Y.-Y. Xu, L.-H. Yu, Z. Mo, F. Gong, X.-L. Zhang, W.-G. Tian, L. Hu, X.-X. Zhang, J.-L. Xiang, H.-X. Du, H.-W. Liu, C.-H. Lang, X.-H. Luo, S.-B. Wu, X.-P. Cui, Z. Zhou, M.-M. Zhu, J. Wang, C.-J. Xue, X.-F. Li, L. Wang, Z.-J. Li, K. Wang, C.-C. Niu, Q.-J. Yang, X.-J. Tang, Y. Zhang, X.-M. Liu, J.-J. Li, D.-C. Zhang, F. Zhang, P. Liu, J. Yuan, Q. Li, J.-L. Hu, J. Chen, A.-L. Huang, Antibody responses to SARS-CoV-2 in patients with COVID-19, Nat. Med. 26 (2020) 845–848, https://doi.org/10.1038/s41591-020-0897-1.

[2] K. Li, B. Huang, M. Wu, A. Zhong, L. Li, Y. Cai, Z. Wang, L. Wu, M. Zhu, J. Li, Z. Wang, W. Wu, W. Li, B. Bosco, Z. Gan, Q. Qiao, J. Wu, Q. Wang, S. Wang, X. Xia, Dynamic changes in anti-SARS-CoV-2 antibodies during SARS-CoV-2 infection and recovery from COVID-19, Nat. Commun. 11 (2020) 6044, https://doi.org/10.1038/s41467-020-19943-y.

[3] K. Murphy, C. Weaver, Integrated dynamics of innate and adaptive immunity, in: Janeway's Immunobiology, 9th edition, Garland Science, Taylor & Francis Group, New York and London, 2017, pp. 445–491.

[4] M. Aguilar-Bretones, B.M. Westerhuis, M.P. Raadsen, E. de Bruin, F.D. Chandler, N. M. Okba, B.L. Haagmans, T. Langerak, H. Endeman, J.P. van den Akker, D. A. Gommers, E.C. van Gorp, C.H. GeurtsvanKessel, R.D. de Vries, R.A. Fouchier, B. H. Rockx, M.P. Koopmans, G.P. van Nierop, Seasonal coronavirus-specific B cells with limited SARS-CoV-2 cross-reactivity dominate the IgG response in severe COVID-19, J. Clin. Invest. 131 (2021), https://doi.org/10.1172/jci150613.

[5] A. Grifoni, D. Weiskopf, S.I. Ramirez, J. Mateus, J.M. Dan, C.R. Moderbacher, S. A. Rawlings, A. Sutherland, L. Premkumar, R.S. Jadi, D. Marrama, A.M. de Silva, A. Frazier, A.F. Carlin, J.A. Greenbaum, B. Peters, F. Krammer, D.M. Smith, S. Crotty, A. Sette, Targets of T cell responses to SARS-CoV-2 coronavirus in humans with COVID-19 disease and unexposed individuals, Cell 181 (2020) 1489–1501, e15, https://doi.org/10.1016/j.cell.2020.05.015.

[6] A.G. Dykema, B. Zhang, B.A. Woldemeskel, C.C. Garliss, L.S. Cheung, D. Choudhury, J. Zhang, L. Aparicio, S. Bom, R. Rashid, J.X. Caushi, E.H.-C. Hsiue, K. Cascino, E.A. Thompson, A.K. Kwaa, D. Singh, S. Thapa, A.A. Ordonez, A. Pekosz, F.R. D'Alessio, J.D. Powell, S. Yegnasubramanian, S. Zhou, D.M. Pardoll, H. Ji, A.L. Cox, J.N. Blankson, K.N. Smith, Functional characterization of CD4+ T-cell receptors cross-reactive for SARS-CoV-2 and endemic coronaviruses, J. Clin. Invest. 131 (2021), https://doi.org/10.1172/jci146922.

[7] E.M. Anderson, E.C. Goodwin, A. Verma, C.P. Arevalo, M.J. Bolton, M.E. Weirick, S. Gouma, C.M. McAllister, S.R. Christensen, J. Weaver, P. Hicks, T.B. Manzoni, O. Oniyide, H. Ramage, D. Mathew, A.E. Baxter, D.A. Oldridge, A.R. Greenplate, J.E. Wu, C. Alanio, K. D'Andrea, O. Kuthuru, J. Dougherty, A. Pattekar, J. Kim, N. Han, S.A. Apostolidis, A.C. Huang, L.A. Vella, L. Kuri-Cervantes, M.B. Pampena, T.Up.C. P. Unit, M.R. Betts, E.J. Wherry, N.J. Meyer, S. Cherry, P. Bates, D.J. Rader, S.E. Hensley, Seasonal human coronavirus antibodies are boosted upon SARS-CoV-2 infection but not associated with protection, Cell 184 (2021) 1858–1864.e10. doi: https://doi.org/10.1016/j.cell.2021.02.010.

[8] T. Aydillo, A. Rombauts, D. Stadlbauer, S. Aslam, G. Abelenda-Alonso, A. Escalera, F. Amanat, K. Jiang, F. Krammer, J. Carratala, A. García-Sastre, Immunological imprinting of the antibody response in COVID-19 patients, Nat. Commun. 12 (2021) 3781, https://doi.org/10.1038/s41467-021-23977-1.

[9] K. Röltgen, S.C.A. Nielsen, O. Silva, S.F. Younes, M. Zaslavsky, C. Costales, F. Yang, O.F. Wirz, D. Solis, R.A. Hoh, A. Wang, P.S. Arunachalam, D. Colburg, S. Zhao, E. Haraguchi, A.S. Lee, M.M. Shah, M. Manohar, I. Chang, F. Gao, V. Mallajosyula, C. Li, J. Liu, M.J. Shoura, S.B. Sindher, E. Parsons, N.J. Dashdorj, N.D. Dashdorj, R. Monroe, G.E. Serrano, T.G. Beach, R.S. Chinthrajah, G.W. Charville, J.L. Wilbur, J.N. Wohlstadter, M.M. Davis, B. Pulendran, M.L. Troxell, G.B. Sigal, Y. Natkunam, B.A. Pinsky, K.C. Nadeau, S.D. Boyd, Immune imprinting, breadth of variant recognition, and germinal center response in human SARS-CoV-2 infection and vaccination, Cell 185 (2022) 1025–1040, e14, https://doi.org/10.1016/j.cell.2022.01.018.

[10] A.L. McNaughton, R.S. Paton, M. Edmans, J. Youngs, J. Wellens, P. Phalora, A. Fyfe, S. Belij-Rammerstorfer, J.S. Bolton, J. Ball, G.W. Carnell, W. Dejnirattisai, C. Dold, D.W. Eyre, P. Hopkins, A. Howarth, K. Kooblall, H. Klim, S. Leaver, L. N. Lee, C. López-Camacho, S.F. Lumley, D.C. Macallan, A.J. Mentzer, N.M. Provine, J. Ratcliff, J. Slon-Compos, D. Skelly, L. Stolle, P. Supasa, N. Temperton, C. Walker, B. Wang, D. Wyncoll, O.P.T.C.I. for C.-19 (OPTIC) consortium, S.N.B.T.S. (SNBTS) consortium, P. Simmonds, T. Lambe, J.K. Baillie, M.G. Semple, P.J. Openshaw, I.S. A.R. and emerging I.C.C.C.C.C. (ISARIC4C) investigators, U. Obolski, M. Turner, M. Carroll, J. Mongkolsapaya, G. Screaton, S.H. Kennedy, L. Jarvis, E. Barnes, S. Dunachie, J. Lourenço, P.C. Matthews, T. Bicanic, P. Klenerman, S. Gupta, C. P. Thompson, Fatal COVID-19 outcomes are associated with an antibody response targeting epitopes shared with endemic coronaviruses, JCI Insight 7 (2022), https://doi.org/10.1172/jci.insight.156372.

[11] T.S. Johnston, S.H. Li, M.M. Painter, R.K. Atkinson, N.R. Douek, D.B. Reeg, D. C. Douek, E.J. Wherry, S.E. Hensley, Immunological imprinting shapes the specificity of human antibody responses against SARS-CoV-2 variants, Immunity 57 (2024) 912–925.e4, https://doi.org/10.1016/j.immuni.2024.02.017.

[12] WHO, R&D Blueprint Novel Coronavirus, COVID-19 Therapeutic Trial Synopsis. Appendix 1, 2020.

[13] Y. Cáceres-Martell, D. Fernández-Soto, C. Campos-Silva, E.M. García-Cuesta, J. M. Casasnovas, D. Navas-Herrera, A. Beneítez-Martínez, P. Martínez-Fleta, A. Alfranca, F. Sánchez-Madrid, G. Escudero-López, C. Vilches, R. Jara-Acevedo, H. T. Reyburn, J.M. Rodríguez-Frade, M. Valés-Gómez, Single-reaction multi-antigen serological test for comprehensive evaluation of SARS-CoV-2 patients by flow cytometry, Eur. J. Immunol. 51 (2021) 2633–2640, https://doi.org/10.1002/eji.202149319.

[14] P. Bastard, L.B. Rosen, Q. Zhang, E. Michailidis, H.-H. Hoffmann, Y. Zhang, K. Dorgham, Q. Philippot, J. Rosain, V. Béziat, J. Manry, E. Shaw, L. Haljasmägi, P. Peterson, L. Lorenzo, L. Bizien, S. Trouillet-Assant, K. Dobbs, A.A. de Jesus, A. Belot, A. Kallaste, E. Catherinot, Y. Tandjaoui-Lambiotte, J.L. Pen, G. Kerner, B. Bigio, Y. Seeleuthner, R. Yang, A. Bolze, A.N. Spaan, O.M. Delmonte, M.S. Abers, A. Aiuti, G. Casari, V. Lampasona, L. Piemonti, F. Ciceri, K. Bilguvar, R.P. Lifton, M. Vasse, D.M. Smadja, M. Migaud, J. Hadjadj, B. Terrier, D. Duffy, L. Quintana-Murci, D. van de Beek, L. Roussel, D.C. Vinh, S.G. Tangye, F. Haerynck, D. Dalmau, J. Martinez-Picado, P. Brodin, M.C. Nussenzweig, S. Boisson-Dupuis, C. Rodríguez-Gallego, G. Vogt, T.H. Mogensen, A.J. Oler, J. Gu, P.D. Burbelo, J.I. Cohen, A. Biondi, L.R. Bettini, M. D'Angio, P. Bonfanti, P. Rossignol, J. Mayaux, F. Rieux-Laucat, E.S. Husebye, F. Fusco, M.V. Ursini, L. Imberti, A. Sottini, S. Paghera, E. Quiros-Roldan, C. Rossi, R. Castagnoli, D. Montagna, A. Licari, G.L. Marseglia, X. Duval, J. Ghosn, J.S. Tsang, R. Goldbach-Mansky, K. Kisand, M.S. Lionakis, A. Puel, S.-Y. Zhang, S.M. Holland, G. Gorochov, E. Jouanguy, C.M. Rice, A. Cobat, L.D. Notarangelo, L. Abel, H.C. Su, J.-L. Casanova, A.A. Arias, B. Boisson, S. Boucherit, J. Bustamante, M. Chbihi, J. Chen, M. Chrabieh, T. Kochetkov, T. L. Voyer, D. Liu, Y. Nemirovskaya, M. Ogishi, D. Papandrea, C. Patissier, F. Rapaport, M. Roynard, N. Vladikine, M. Woollett, P. Zhang, A. Kashyap, L. Ding, M. Bosticardo, Q. Wang, S. Ochoa, H. Liu, S.D. Chauvin, M. Stack, G. Koroleva,

N. Bansal, C.L. Dalgard, A.L. Snow, J. Abad, S. Aguilera-Albesa, O.M. Akcan, I. A. Darazam, J.C. Aldave, M.A. Ramos, S.A. Nadji, G. Alkan, J. Allardet-Servent, L. M. Allende, L. Alsina, M.-A. Alyanakian, B. Amador-Borrero, Z. Amoura, A. Antolí, S. Arslan, S. Assant, T. Auguet, A. Azot, F. Bajolle, A. Baldolli, M. Ballester, H. B. Feldman, B. Barrou, A. Beurton, A. Bilbao, G. Blanchard-Rohner, I. Blanco, A. Blandinières, D. Blazquez-Gamero, M. Bloomfield, M. Bolivar-Prados, R. Borie, A.A. Bousfiha, C. Bouvattier, O. Boyarchuk, M.R.P. Bueno, J. Bustamante, J.J. C. Agra, S. Calimli, R. Capra, M. Carrabba, C. Casasnovas, M. Caseris, M. Castelle, F. Castelli, M.C. de Vera, M.V. Castro, E. Catherinot, M. Chalumeau, B. Charbit, M. P. Cheng, P. Clavé, B. Clotet, A. Codina, F. Colkesen, F. Colkesen, R. Colobran, C. Comarmond, A.G. Corsico, D. Dalmau, D.R. Darley, N. Dauby, S. Dauger, L. de Pontual, A. Dehban, G. Delplancq, A. Demoule, A.D. Sabatino, J.-L. Diehl, S. Dobbelaere, S. Durand, W. Eldars, M. Elgamal, M.H. Elnagdy, M. Emiroglu, E. H. Erdeniz, S.E. Aytekin, R. Euvrard, R. Evcen, G. Fabio, L. Faivre, A. Falck, M. Fartoukh, M. Faure, M.F. Arquero, C. Flores, B. Francois, V. Fumadó, F. Fusco, B.G. Solis, P. Gaussem, J. Gil-Herrera, L. Gilardin, M.G. Alarcon, M. Girona-Alarcón, J.-C. Goffard, F. Gok, R. González-Montelongo, A. Guerder, Y. Gul, S. N. Guner, M. Gut, J. Hadjadj, F. Haerynck, R. Halwani, L. Hammarström, N. Hatipoglu, E. Hernandez-Brito, M.S. Holanda-Peña, J.P. Horcajada, S. Hraiech, L. Humbert, A.D. Iglesias, A. Íñigo-Campos, M. Jamme, M.J. Arranz, I. Jordan, F. Kanat, H. Kapakli, I. Kara, A. Karbuz, K.K. Yasar, S. Keles, Y.K. Demirkol, A. Klocperk, Z.J. Król, P. Kuentz, Y.W.M. Kwan, J.-C. Lagier, Y.-L. Lau, F. L. Bourgeois, Y.-S. Leo, R.L. Lopez, D. Leung, M. Levin, M. Lévy, R. Lévy, Z. Li, A. Linglart, J.M. Lorenzo-Salazar, C. Louapre, C. Lubetzki, C.-E. Luyt, D.C. Lye, D. Mansouri, M. Marjani, J.M. Pereira, A. Martin, D.M. Pueyo, J. Martinez-Picado, I. Marzana, A. Mathian, L.R.B. Matos, G.V. Matthews, J. Mayaux, J.-L. Mège, I. Melki, J.-F. Meritet, O. Metin, I. Meyts, M. Mezidi, I. Migeotte, M. Millereux, T. Mirault, C. Mircher, M. Mirsaeidi, A.M. Melián, A.M. Martinez, P. Morange, C. Mordacq, G. Morelle, S. Mouly, A. Muñoz-Barrera, C. Nafati, J.F. Neves, L.F. P. Ng, Y.N. Medina, E.N. Cuadros, J.G. Ocejo-Vinyals, Z. Orbak, M. Oualha, T. Özçelik, Q.P. Hammarström, C. Parizot, T. Pascreau, E. Paz-Artal, R.P. de Diego, A. Philippe, Q. Philippot, L. Planas-Serra, D. Ploin, J. Poissy, G. Poncelet, M. Pouletty, P. Quentric, D. Raoult, A.-S. Rebillat, I. Reisli, P. Ricart, J.-C. Richard, N. Rivet, J.G. Rivière, G.R. Blanch, C. Rodrigo, C. Rodriguez-Gallego, A. Rodríguez-Palmero, C.S. Romero, A. Rothenbuhler, F. Rozenberg, M.Y.R. del Prado, J.S. Riera, O. Sanchez, S. Sánchez-Ramón, A. Schluter, M. Schmidt, C.E. Schweitzer, F. Scolari, A. Sediva, L.M. Seijo, D. Sene, S. Senoglu, M.R.J. Seppänen, A.S. Ilovich, M. Shahrooei, D. Smadja, A. Sobh, X.S. Moreno, J. Solé-Violán, C. Soler, P. Soler-Palacín, Y. Stepanovskiy, A. Stoclin, F. Taccone, Y. Tandjaoui-Lambiotte, J.-L. Taupin, S.J. Tavernier, B. Terrier, C. Thumerelle, G. Tomasoni, J. Toubiana, J. T. Alvarez, S. Trouillet-Assant, J. Troya, A. Tucci, M.V. Ursini, Y. Uzunhan, P. Vabres, J. Valencia-Ramos, A.M.V.D. Rym, I. Vandernoot, H. Vatansev, V. Vélez-Santamaria, S. Viel, C. Vilain, M.E. Vilaire, A. Vincent, G. Voiriot, F. Vuotto, A. Yosunkaya, B.E. Young, F. Yucel, F. Zannad, M. Zatz, A. Belot, G. Foti, G. Bellani, G. Citerio, E. Contro, A. Pesci, M.G. Valsecchi, M. Cazzaniga, C. Bole-Feysot, S. Lyonnet, C. Masson, P. Nitschke, A. Pouliet, Y. Schmitt, F. Tores, M. Zarhrate, L. Abel, C. Andrejak, F. Angoulvant, D. Bachelet, R. Basmaci, S. Behillil, M. Beluze, D. Benkerrou, K. Bhavsar, F. Bompart, L. Bouadma, M. Bouscambert, M. Caralp, M. Cervantes-Gonzalez, A. Chair, A. Coelho, C. Couffignal, S. Couffin-Cadiergues, E. D'ortenzio, C.D. Silveira, M.-P. Debray, D. Deplanque, D. Descamps, M. Desvallées, A. Diallo, A. Diouf, C. Dorival, F. Dubos, X. Duval, P. Eloy, V.V. E. Enouf, H. Esperou, M. Esposito-Farese, M. Etienne, N. Ettalhaoui, N. Gault, A. Gaymard, J. Ghosn, T. Gigante, I. Gorenne, J. Guedj, A. Hoctin, I. Hoffmann, S. Jaafoura, O. Kafif, F. Kaguelidou, S. Kali, A. Khalil, C. Khan, C. Laouénan, S. Laribi, M. Le, Q.L. Hingrat, S.L. Mestre, H.L. Nagard, F.-X. Lescure, Y. Lévy, C. Levy-Marchal, B. Lina, G. Lingas, J.C. Lucet, D. Malvy, M. Mambert, F. Mentré, N. Mercier, A. Meziane, H. Mouquet, J. Mullaert, N. Neant, M. Noret, J. Pages, A. Papadopoulos, C. Paul, N. Peiffer-Smadja, V. Petrov-Sanchez, G. Peytavin, O. Picone, O. Puéchal, M. Rosa-Calatrava, B. Rossignol, P. Rossignol, C. Roy, M. Schneider, C. Semaille, N.S. Mohammed, L. Tagherset, C. Tardivon, M.-C. Tellier, F. Téoulé, O. Terrier, J.-F. Timsit, T. Treoux, C. Tual, S. Tubiana, S. van der Werf, N. Vanel, A. Veislinger, B. Visseaux, A. Wiedemann, Y. Yazdanpanah, L. Abel, A. Alcover, H. Aschard, K. Astrom, P. Bousso, P. Bruhns, A. Cumano, C. Demangel, L. Deriano, J.D. Santo, F. Dromer, G. Eberl, J. Enninga, J. Fellay, I. Gomperts-Boneca, M. Hasan, S. Hercberg, O. Lantz, H. Mouquet, E. Patin, S. Pellegrini, S. Pol, A. Rausell, L. Rogge, A. Sakuntabhai, O. Schwartz, B. Schwikowski, S. Shorte, F. Tangy, A. Toubert, M. Touvier, M.-N. Ungeheuer, M. L. Albert, D. Duffy, L. Quintana-Murci, L. Alavoine, K.K.A. Amat, S. Behillil, J. Bielicki, P. Bruijning, C. Burdet, E. Caumes, C. Charpentier, B. Coignard, Y. Costa, S. Couffin-Cadiergues, F. Damond, A. Dechanet, C. Delmas, D. Descamps, X. Duval, J.-L. Ecobichon, V. Enouf, H. Espérou, W. Frezouls, N. Houhou, E. Ilic-Habensus, O. Kafif, J. Kikoine, Q.L. Hingrat, D. Lebeaux, A. Leclercq, J. Lehacaut, S. Letrou, B. Lina, J.-C. Lucet, D. Malvy, P. Manchon, M. Mandic, M. Meghadecha, J. Motiejunaite, M. Nouroudine, V. Piquard, A. Postolache, C. Quintin, J. Rexach, L. Roufai, Z. Terzian, M. Thy, S. Tubiana, S. van der Werf, V. Vignali, B. Visseaux, Y. Yazdanpanah, M. van Agtmael, A.G. Algera, F. van Baarle, D. Bax, M. Beudel, H. J. Bogaard, M. Bomers, L. Bos, M. Botta, J. de Brabander, G. Bree, M.C. Brouwer, S. de Bruin, M. Bugiani, E. Bulle, O. Chouchane, A. Cloherty, P. Elbers, L. Fleuren, S. Geerlings, B. Geerts, T. Geijtenbeek, A. Girbes, B. Goorhuis, M.P. Grobusch, F. Hafkamp, L. Hagens, J. Hamann, V. Harris, R. Hemke, S.M. Hermans, L. Heunks, M.W. Hollmann, J. Horn, J.W. Hovius, M.D. de Jong, R. Koning, N. van Mourik, J. Nellen, F. Paulus, E. Peters, T. van der Poll, B. Preckel, J.M. Prins, J. Raasveld, T. Reijnders, M. Schinkel, M.J. Schultz, A. Schuurman, K. Sigaloff, M. Smit, C. S. Stijnis, W. Stilma, C. Teunissen, P. Thoral, A. Tsonas, M. van der Valk, D. Veelo, A.P.J. Vlaar, H. de Vries, M. van Vugt, W.J. Wiersinga, D. Wouters, A.H. (Koos) Zwinderman, D. van de Beek, L. Abel, A. Aiuti, S.A. Muhsen, F. Al-Mulla, M. S. Anderson, A.A. Arias, H.B. Feldman, D. Bogunovic, A. Bolze, A. Bondarenko, A. A. Bousfiha, P. Brodin, Y. Bryceson, C.D. Bustamante, M. Butte, G. Casari, S. Chakravorty, J. Christodoulou, E. Cirulli, A. Condino-Neto, M.A. Cooper, C. L. Dalgard, J.L. DeRisi, M. Desai, B.A. Drolet, S. Espinosa, J. Fellay, C. Flores, J. L. Franco, P.K. Gregersen, F. Haerynck, D. Hagin, R. Halwani, J. Heath, S. E. Henrickson, E. Hsieh, K. Imai, Y. Itan, T. Karamitros, K. Kisand, C.-L. Ku, Y.-L. Lau, Y. Ling, C.L. Lucas, T. Maniatis, D. Mansouri, L. Marodi, I. Meyts, J. D. Milner, K. Mironska, T. Mogensen, T. Morio, L.F.P. Ng, L.D. Notarangelo, G. Novelli, A. Novelli, C. O'Farrelly, S. Okada, T. Ozcelik, R.P. de Diego, A. M. Planas, C. Prando, A. Pujol, L. Quintana-Murci, L. Renia, A. Renieri, C. Rodríguez-Gallego, V. Sancho-Shimizu, V. Sankaran, K.S. Barrett, M. Shahrooei, A. Snow, P. Soler-Palacín, A.N. Spaan, S. Tangye, S. Turvey, F. Uddin, M.J. Uddin, D. van de Beek, S.E. Vazquez, D.C. Vinh, H. von Bernuth, N. Washington, P. Zawadzki, H.C. Su, J.-L. Casanova, Autoantibodies against type I IFNs in patients with life-threatening COVID-19, Science 370 (2020) eabd4585, https://doi.org/10.1126/science.abd4585.

[15] M.A. Fernandez, H. Alzayat, M.C. Jaimes, Y. Kharraz, G. Requena, P. Mendez, Single-cell protein analysis, methods and protocols, Methods Mol. Biol. 2386 (2022) C1–C3, https://doi.org/10.1007/978-1-0716-1771-7_18.

[16] C. Andrés, M. Piñana, B. Borràs-Bermejo, A. González-Sánchez, D. García-Cehic, J. Esperalba, A. Rando, R.-G. Zules-Oña, C. Campos, M.G. Codina, A. Blanco-Grau, S. Colomer-Castell, M.C. Martín, C. Castillo, K. García-Comuñas, R. Vásquez-Mercado, R. Martins-Martins, N. Saubi, M. Campins-Martí, T. Pumarola, J. Quer, A. Antón, A year living with SARS-CoV-2: an epidemiological overview of viral lineage circulation by whole-genome sequencing in Barcelona city (Catalonia, Spain), Emerg. Microbes Infect. 11 (2022) 172–181, https://doi.org/10.1080/22221751.2021.2011617.

[17] D. Goldblatt, G. Alter, S. Crotty, S.A. Plotkin, Correlates of protection against SARS-CoV-2 infection and COVID-19 disease, Immunol. Rev. 310 (2022) 6–26, https://doi.org/10.1111/imr.13091.

[18] J. Sun, E.J. Pearce, Suppression of early IL-4 production underlies the failure of CD4 T cells activated by TLR-stimulated dendritic cells to differentiate into Th2 cells, J. Immunol. 178 (2007) 1635–1644, https://doi.org/10.4049/jimmunol.178.3.1635.

[19] T.J. Fry, C.L. Mackall, The many faces of IL-7: from lymphopoiesis to peripheral T cell maintenance, J. Immunol. 174 (2005) 6571–6576, https://doi.org/10.4049/jimmunol.174.11.6571.

[20] A. Sánchez-Montalvá, D. Álvarez-Sierra, M. Martínez-Gallo, J. Perurena-Prieto, I. Arrese-Muñoz, J.C. Ruiz-Rodríguez, J. Espinosa-Pereiro, P. Bosch-Nicolau, X. Martínez-Gómez, A. Antón, F. Martínez-Valle, M. Riveiro-Barciela, A. Blanco-Grau, F. Rodríguez-Frias, P. Castellano-Escuder, E. Poyatos-Canton, J. Bas-Minguet, E. Martínez-Cáceres, A. Sánchez-Pla, C. Zurera-Egea, A. Teniente-Serra, M. Hernández-González, R. Pujol-Borrell, A.L. Uriel, R. Dieli, R. Colobran, G. Codina, T. Pumarola, R. Ferrer, V. Cortina, M. Campins, I. Ruiz, N. Fernaíndez, E. Ribera, J. Roig, R. Ferrer, A. Ruiz-Sanmartín, A. Selva, M. Labrador, M.J. S. Romeo, J. Ferrer, E. Polverino, A. Alvarez, M.Q. Gorgas, M. Miarons, P. Soler-Palacin, A. Martin, A. Suy, M.J. Buzón, M. Genescà, S. Perez-Hoyos, M. Mota-Foix, Exposing and overcoming limitations of clinical laboratory tests in COVID-19 by adding immunological parameters; a retrospective cohort analysis and pilot study, Front. Immunol. 13 (2022) 902837, https://doi.org/10.3389/fimmu.2022.902837.

[21] S.A. Lauer, K.H. Grantz, Q. Bi, F.K. Jones, Q. Zheng, H.R. Meredith, A.S. Azman, N. G. Reich, J. Lessler, The incubation period of coronavirus disease 2019 (COVID-19) from publicly reported confirmed cases: estimation and application, Ann. Intern. Med. 172 (2020), https://doi.org/10.7326/m20-0504. M20-0504.

[22] S. Crotty, T follicular helper cell biology: a decade of discovery and diseases, Immunity 50 (2019) 1132–1148, https://doi.org/10.1016/j.immuni.2019.04.011.

[23] X. Wang, M.A. Sanborn, Y. Dai, J. Rehman, Temporal transcriptomic analysis using TrendCatcher identifies early and persistent neutrophil activation in severe COVID-19, JCI Insight 7 (2022), https://doi.org/10.1172/jci.insight.157255.

[24] Y.M. Mueller, T.J. Schrama, R. Ruijten, M.W.J. Schreurs, D.G.B. Grashof, H.J. G. van de Werken, G.J. Lasinio, D. Álvarez-Sierra, C.H. Kiernan, M.D.C. Eiro, M. van Meurs, I. Brouwers-Haspels, M. Zhao, L. Li, H. de Wit, C.A. Ouzounis, M.E. P. Wilmsen, T.M. Alofs, D.A. Laport, T. van Wees, G. Kraker, M.C. Jaimes, S. V. Bockstael, M. Hernández-González, C. Rokx, B.J.A. Rijnders, R. Pujol-Borrell, P. D. Katsikis, Stratification of hospitalized COVID-19 patients into clinical severity progression groups by immuno-phenotyping and machine learning, Nat. Commun. 13 (2022) 915, https://doi.org/10.1038/s41467-022-28621-0.

[25] L. Wynants, B.V. Calster, G.S. Collins, R.D. Riley, G. Heinze, E. Schuit, M.M. J. Bonten, J.A.A. Damen, T.P.A. Debray, M.D. Vos, P. Dhiman, M.C. Haller, M. O. Harhay, L. Henckaerts, N. Kreuzberger, A. Lohmann, K. Luijken, J. Ma, C.L. A. Navarro, J.B. Reitsma, J.C. Sergeant, C. Shi, N. Skoetz, L.J.M. Smits, K.I.E. Snell, M. Sperrin, R. Spijker, E.W. Steyerberg, T. Takada, S.M.J.V. Kuijk, F.S.V. Royen, C. Wallisch, L. Hooft, K.G.M. Moons, M.V. Smeden, Prediction models for diagnosis and prognosis of covid-19: systematic review and critical appraisal, BMJ 369 (2020), https://doi.org/10.1136/bmj.m1328.

[26] J.W. Yewdell, J.J.S. Santos, Original antigenic sin: how original? How sinful? Cold Spring Harb. Perspect. Med. 11 (2020) a038786 https://doi.org/10.1101/cshperspect.a038786.

[27] W. Fierz, B. Walz, Antibody dependent enhancement due to original antigenic sin and the development of SARS, Front. Immunol. 11 (2020) 1120, https://doi.org/10.3389/fimmu.2020.01120.

[28] M. Aguilar-Bretones, R.A. Fouchier, M.P. Koopmans, G.P. van Nierop, Impact of antigenic evolution and original antigenic sin on SARS-CoV-2 immunity, J. Clin. Invest. 133 (2023) e162192, https://doi.org/10.1172/jci162192.

[29] J. Mateus, A. Grifoni, A. Tarke, J. Sidney, S.I. Ramirez, J.M. Dan, Z.C. Burger, S. A. Rawlings, D.M. Smith, E. Phillips, S. Mallal, M. Lammers, P. Rubiro, L. Quiambao, A. Sutherland, E.D. Yu, R.S. da Antunes, J. Greenbaum, A. Frazier, A. J. Markmann, L. Premkumar, A. de Silva, B. Peters, S. Crotty, A. Sette, D. Weiskopf, Selective and cross-reactive SARS-CoV-2 T cell epitopes in unexposed humans, Science 370 (2020) 89–94, https://doi.org/10.1126/science.abd3871.

[30] A. Sette, J. Sidney, S. Crotty, T cell responses to SARS-CoV-2, Annu. Rev. Immunol. 41 (2023) 343–373, https://doi.org/10.1146/annurev-immunol-101721-061120.

[31] R.T. Suhandynata, M.A. Hoffman, M.J. Kelner, R.W. McLawhon, S.L. Reed, R. L. Fitzgerald, Longitudinal monitoring of SARS-CoV-2 IgM and IgG seropositivity to detect COVID-19, J. Appl. Lab. Med. 5 (2020) 908–920, https://doi.org/10.1093/jalm/jfaa079.

[32] H. Verkerke, M. Horwath, B. Saeedi, D. Boyer, J.W. Allen, J. Owens, C.M. Arthur, H. Nakahara, J. Rha, K. Patel, S.-C. Wu, A. Paul, N. Yasin, J. Wang, S. Shin, D. Brown, K. Normile, L. Cole, M. Meyers, H. Lin, E. Woods, J. Isaac, K. Broder, J. Wade, R.C. Kauffman, R. Patel, C.D. Josephson, S. Reynolds, M. Sherman, J. Wrammert, D. Alter, J. Guarner, J.D. Roback, A. Neish, S.R. Stowell, Comparison of antibody class-specific SARS-CoV-2 serologies for the diagnosis of acute COVID-19, J. Clin. Microbiol. 59 (2021), https://doi.org/10.1128/jcm.02026-20 e02026-20.

[33] A.E. Oja, B. Piet, C. Helbig, R. Stark, D. van der Zwan, H. Blaauwgeers, E.B. M. Remmerswaal, D. Amsen, R.E. Jonkers, P.D. Moerland, M.A. Nolte, R.A.W. van Lier, P. Hombrink, Trigger-happy resident memory CD4+ T cells inhabit the human lungs, Mucosal Immunol. 11 (2018) 654–667, https://doi.org/10.1038/mi.2017.94.

[34] J. Grau-Expósito, N. Sánchez-Gaona, N. Massana, M. Suppi, A. Astorga-Gamaza, D. Perea, J. Rosado, A. Falcó, C. Kirkegaard, A. Torrella, B. Planas, J. Navarro, P. Suanzes, D. Álvarez-Sierra, A. Ayora, I. Sansano, J. Esperalba, C. Andrés, A. Antón, S.R.Y. Cajal, B. Almirante, R. Pujol-Borrell, V. Falcó, J. Burgos, M. J. Buzón, M. Genescà, Peripheral and lung resident memory T cell responses against SARS-CoV-2, Nat. Commun. 12 (2021) 3010, https://doi.org/10.1038/s41467-021-23333-3.

[35] C. Gregoire, L. Spinelli, S. Villazala-Merino, L. Gil, M.P. Holgado, M. Moussa, C. Dong, A. Zarubica, M. Fallet, J.-M. Navarro, B. Malissen, P. Milpied, M. Gaya, Viral infection engenders bona fide and bystander subsets of lung-resident memory B cells through a permissive mechanism, Immunity 55 (2022) 1216–1233, e9, https://doi.org/10.1016/j.immuni.2022.06.002.

[36] M.S. Suthar, M.G. Zimmerman, R.C. Kauffman, G. Mantus, S.L. Linderman, W. H. Hudson, A. Vanderheiden, L. Nyhoff, C.W. Davis, O. Adekunle, M. Affer, M. Sherman, S. Reynolds, H.P. Verkerke, D.N. Alter, J. Guarner, J. Bryksin, M. C. Horwath, C.M. Arthur, N. Saakadze, G.H. Smith, S. Edupuganti, E.M. Scherer, K. Hellmeister, A. Cheng, J.A. Morales, A.S. Neish, S.R. Stowell, F. Frank, E. Ortlund, E.J. Anderson, V.D. Menachery, N. Rouphael, A.K. Mehta, D. S. Stephens, R. Ahmed, J.D. Roback, J. Wrammert, Rapid generation of neutralizing antibody responses in COVID-19 patients, Cell Rep. Med. 1 (2020) 100040, https://doi.org/10.1016/j.xcrm.2020.100040.

[37] N. Baumgarth, Original antigenic sin: not so sinful after all, Trends Immunol. 44 (2023) 487–489, https://doi.org/10.1016/j.it.2023.05.010.